Separation of Q_β and Q_γ Charge Components in Frog Cut Twitch Fibers with Tetracaine

Critical Comparison with Other Methods

CHIU SHUEN HUI and WEI CHEN

From the Department of Physiology and Biophysics, Indiana University Medical Center, Indianapolis, Indiana 46202

ABSTRACT Charge movement was measured in frog cut twitch fibers with the double Vaseline-gap technique. 25 μM tetracaine had very little effect on the maximum amounts of Q_β and Q_γ but slowed the kinetics of the I_γ humps in the ON segments of TEST-minus-CONTROL current traces, giving rise to biphasic transients in the difference traces. This concentration of tetracaine also shifted $\overline{V}_\gamma$ 3.7 (SEM 0.7) mV in the depolarizing direction, resulting in a difference Q-V plot that was bell-shaped with a peak at ~ -50 mV. 0.5–1.0 mM tetracaine suppressed the total amount of charge. The suppressed component had a sigmoidal voltage distribution with $\overline{V} = -56.6$ (SEM 1.1) mV, $k = 2.5$ (SEM 0.5) mV, and $q_{max}/c_m = 9.2$ (SEM 1.5) nC/μF, suggesting that the tetracaine-sensitive charge had a steep voltage dependence, a characteristic of the Q_γ component. An intermediate concentration (0.1–0.5 mM) of tetracaine shifted $\overline{V}_\gamma$ and partially suppressed the tetracaine-sensitive charge, resulting in a difference Q-V plot that rose to a peak and then decayed to a plateau level. Following a TEST pulse to > -60 mV, the slow inward current component during a post-pulse to ~ -60 mV was also tetracaine sensitive. The voltage distribution of the charge separated by tetracaine (method 1) was compared with those separated by three other existing methods: (*a*) the charge associated with the hump component separated by a sum of two kinetic functions from the ON segment of a TEST-minus-CONTROL current trace (method 2), (*b*) the steeply voltage-dependent component separated from a Q-V plot of the total charge by fitting with a sum of two Boltzmann distribution functions (method 3), and (*c*) the sigmoidal component separated from the Q-V plot of the final OFF charge obtained with a two-pulse protocol (method 4). The steeply voltage-dependent components separated by all four methods are consistent with each other, and are therefore concluded to be equivalent to the same Q_γ component. The

Address reprint requests to Dr. Chiu Shuen Hui, Department of Physiology and Biophysics, Indiana University Medical Center, 635 Barnhill Drive, Indianapolis, IN 46202.

Dr. Chen's present address is Department of Surgery, University of Chicago, 5841 S. Maryland Ave., Chicago, IL 60637.

J. GEN. PHYSIOL. © The Rockefeller University Press · 0022-1295/92/06/0985/32 $2.00
Volume 99 June 1992 985–1016

shortcomings of each separation method are critically discussed. Since each method has its own advantages and disadvantages, it is recommended that, as much as possible, Q_γ should be separated by more than one method to obtain more reliable results.

INTRODUCTION

It is generally accepted that intramembranous charge movement in skeletal muscle is the voltage sensor for sensing transverse tubule (T-tubule) depolarization and its movement triggers Ca release from the sarcoplasmic reticulum (SR) by a mechanism that remains to be elucidated. Early studies on charge movement in frog intact twitch fibers (Schneider and Chandler, 1973; Adrian and Almers, 1976; Adrian et al., 1976; Chandler et al., 1976*a*, *b*) showed that the current transient flows outward upon depolarization and decays more or less exponentially. Subsequently, under slightly different experimental conditions, a slower, hump-shaped charge movement component was observed in the ON segments of charge movement traces from frog intact fibers (Adrian and Peres, 1977, 1979; Huang, 1982; Hui, 1982, 1983*a*, *b*) and from frog cut fibers (Horowicz and Schneider, 1981; Vergara and Caputo, 1983), but not in the OFF segments. Since then, investigators have been trying to characterize the two charge components and clarify their physiological role(s). Adrian and Peres (1979) defined the early (also earlier in the chronology of discovery) charge movement component as Q_β and the late, hump-shaped component as Q_γ.

Since the Q_γ component of charge movement is more tightly associated with Ca release from the SR or generation of tension than the Q_β component (Hui, 1983*b*), it is of interest to develop a reliable technique to separate Q_γ from the total charge. Unfortunately, different investigators have been using different methods to separate Q_β and Q_γ, thereby introducing different sets of definitions for the notations.

Subsequent to the attempt of Adrian and Peres (1979) to separate Q_β and Q_γ, it was found that Q_β and Q_γ responded differently to agents such as tetracaine (in intact fibers: Huang, 1982; Hui, 1983*a*; in cut fibers: Vergara and Caputo, 1983). These investigators defined the tetracaine-sensitive component as Q_γ and the tetracaine-resistant component as Q_β. In this paper, this separation method will be called method 1. Hui (1983*b*) then developed a mathematical technique based on the original kinetic definitions for Q_β and Q_γ to separate the two components in the ON segments of charge movement traces from intact fibers. This will be called method 2. More recently, Hui and Chandler (1990) separated the two components by fitting the steady-state Q-V plot for the total charge from cut fibers by a sum of two Boltzmann distribution functions with different steepness. They defined the steeper Boltzmann component as Q_γ and the other as Q_β. This will be called method 3. Finally, Hui and Chandler (1991) found that, in cut fibers, the restorations of Q_β and Q_γ to the resting positions upon repolarization to an intermediate potential near −60 mV also have different kinetics. Based on this difference, they dissected the Q_γ component by applying a brief, constant post-pulse to the intermediate potential after each TEST pulse and studied the final OFF charge at −90 mV after the post-pulse. This will be called method 4.

Hui (1983*b*) showed that the Q_γ component dissected out with method 2 in intact fibers is tetracaine sensitive, consistent with the definition of Q_γ in method 1. Hui and

Chandler (1991) showed that the Q_γ component dissected out with method 4 in cut fibers is consistent with the component separated by method 3. Hui (1991*a*) also showed that the separation of Q_β and Q_γ in cut fibers by method 2 is in qualitative agreement with the separation by method 3, but the agreement appears to be poorer in intact fibers. Nonetheless, the equivalences of the Q_β and Q_γ components separated by all four methods have not been fully established.

The first aim of this paper is to study the effect of tetracaine on charge movement in cut fibers. It will be shown that the suppression of charge movement in cut fibers has a different dose–response relationship as compared with that in intact fibers (Huang, 1982; Hui, 1983*a*). The second aim is to compare the four separation methods in the same cut fiber so as to establish an equivalence of the different sets of definitions. In the following paper (Hui and Chen, 1992) it will be shown that the separation of Q_β and Q_γ by making use of their steady-state inactivation properties (Adrian and Peres, 1979) is not equivalent to the separations by the four methods used in this paper.

A preliminary report of some of the findings in this paper has appeared (Chen and Hui, 1989).

METHODS

Solutions

Solution A (relaxing solution): 120 mM K·glutamate, 1 mM $MgSO_4$, 0.1 mM K_2·EGTA, and 5 mM K_2·PIPES, pH 7.0.

Solution B (internal solution): 45.5 mM Cs·glutamate, 20 mM Cs_2·creatine phosphate, 20 mM Cs_2·EGTA, 6.8 mM $MgSO_4$, 5.5 mM Cs_2·ATP, 5 mM glucose, 5 mM Cs_2·PIPES, and 60 μM total Ca, pH 7.0.

Solution C (external solution): 120 mM TEA·Cl, 2.5 mM RbCl, 1.8 mM $CaCl_2$, 2.15 mM Na_2HPO_4, 0.85 mM NaH_2PO_4, and 1 μM tetrodotoxin, pH 7.1.

TEA^+ and Rb^+ in solution C and Cs^+ in solution B were used to minimize K^+ currents. TTX in solution C was for blocking Na^+ current. Solution B contained no added Ca except for the trace amount of Ca present in Cs·glutamate, estimated to be 60 μM. Tetracaine solutions were prepared by adding the appropriate amounts of tetracaine (Sigma Chemical Co., St. Louis, MO) to solution C.

Muscle and Fiber Preparation

Experiments were performed on cut semitendinosus muscle fibers of English frogs, *Rana temporaria*, cold-adapted in a refrigerator at ~4°C. The animals were killed by the conventional decapitation and pithing method. Cut fibers were dissected in solution A following the procedure used by Kovacs et al. (1983) and Irving et al. (1987) and mounted in a double Vaseline-gap chamber (see Fig. 1 of Irving et al., 1987). The two end pools were filled with solution B and the center pool with solution C. Fiber contraction was suppressed by 20 mM $EGTA^{2-}$ in solution B, in addition to stretching to a sarcomere length of 3.5 μm.

Measurement of Charge Movement in Cut Fibers

I_β and I_γ will be used to represent the currents associated with the movements of Q_β and Q_γ. Also, the words control and test will be used to refer to the data taken before and after the

application of tetracaine. They should not be confused with the words CONTROL and TEST used to refer to the traces elicited by CONTROL and TEST pulses.

All experiments were performed at 13–14°C. The experimental protocols were similar to those in previous papers (Chandler and Hui, 1990; Hui and Chandler, 1990). The center pool was kept at virtual ground. Holding potential was set at −90 mV. Three analog signals, V_1, I_2, and V_2 were digitized and stored in a PDP 11/73 microcomputer. V_1 was used for feedback control of membrane potential, which is represented by V throughout. Command pulses were rounded with a time constant of 0.5 ms. A signal-averaged (average of four sweeps) CONTROL current trace, elicited by a CONTROL pulse from −110 to −90 mV, was scaled to subtract the linear capacitive and ionic currents from a single-sweep TEST current trace. All the current traces shown in this paper are TEST-minus-CONTROL current traces without removing the sloping baselines. Each point in a current trace corresponds to 1 ms.

Two different pulse protocols were used in the experiments reported in this paper. For methods 1–3 (see Introduction), each TEST-minus-CONTROL current trace was elicited by a single TEST pulse. This will be referred to as the one-pulse protocol. For method 4, each TEST pulse was immediately followed by a 100-ms post-pulse to a potential around −60 mV. This will be referred to as the two-pulse protocol, which is shown in Fig. 8 *C*. With either protocol, the TEST pulses in a sequence of stimulations were applied in an increasing order of depolarization at a frequency of once per minute.

The principle underlying method 4 has been explained by Hui and Chandler (1991). In essence, I_β and I_γ flow outward during a large depolarizing TEST pulse. On repolarizing briefly to a post-pulse level close to the threshold of Q_γ, parts of Q_β and Q_γ will move back to the resting positions. The remaining parts of Q_β and Q_γ will move back during the final repolarization to the holding potential. Thus, every current trace has three transients, an outward ON current during depolarization, an intermediate inward OFF current during the post-pulse, and a final inward OFF current on repolarization to the holding potential. If the TEST pulse is smaller than the post-pulse, the intermediate current during the post-pulse is an outward ON current, but the final current on repolarization to the holding potential is always an inward OFF current. During the post-pulse period, I_γ has a larger time constant than that of I_β. If the TEST pulse is larger than the post-pulse, the short duration of the post-pulse interrupts the decay of the inward I_γ, which then completes in the final repolarization to the holding potential. Assuming that the brief post-pulse interrupts a constant fraction of Q_γ, then the final OFF charge contains a constant fraction of Q_γ, plus the constant amounts of Q_β and Q_γ that move between the post-pulse potential and the holding potential. Thus, a plot of the final OFF charge as a function of TEST pulse potential shows a sigmoidal component, which is a fraction of the complete Q_γ-V curve, superimposed on a constant pedestal (see Eq. 4 below).

To optimize the detection of the Q_γ component, the potential and the duration of the post-pulse have to be chosen carefully. The potential should be at a level such that the decay of I_γ has the largest time constant and is usually around −65 to −60 mV. This was in fact carefully checked at the beginning of each experiment in which method 4 was applied. The duration of the post-pulse should be long enough to allow as much I_β to decay as possible but not too long to leave too little Q_γ for the final OFF charge. For practical purposes, 100 ms appeared to be an optimal duration of the post-pulse under the conditions of the present experiments.

Data Analysis

In general, OFF charge was used to generate steady-state Q-V plots, whether the one-pulse or two-pulse protocol was used. In some fibers, the OFF charge after a large depolarization was contaminated by an inward tail ionic current (Hui and Chandler, 1990; Hui, 1991*a*, *b*). When the one-pulse protocol was used, the contaminated OFF charge was replaced by the ON charge. When the two-pulse protocol was used, this substitution was not applicable and so the

contaminated OFF charge was excluded from the *Q-V* plot. To make the analysis consistent throughout, points > -30 mV were excluded from all the *Q-V* plots obtained with the two-pulse protocol, although ionic contamination did not occur in every fiber. The restriction is justified because $\overline{V}_\gamma$ generally has a value around -60 to -55 mV, and since k_γ is small, the Q_γ-*V* plot should saturate at < -30 mV, or even < -40 mV.

RESULTS

Effect of Tetracaine on OFF Charge Elicited by a Constant Pulse to −45 mV

The experiment shown in Fig. 1 demonstrates the suppression of charge movement in a cut fiber by different concentrations of tetracaine. Panel *A* shows some representative TEST-minus-CONTROL current traces elicited by identical TEST pulses to -45 mV and panel *B* shows the amounts of OFF charge estimated from all the TEST-minus-CONTROL current traces. The numbered points in *B* correspond to the traces in *A*. Many other traces were recorded at other potentials but are not included in the figure.

The top two traces in Fig. 1 *A* were recorded before the application of tetracaine and serve as control. In the ON segment of trace 1, an outward I_β current rises rapidly in 2–3 ms, but its decay phase is obscured by an I_γ hump, which is extraordinarily prominent for this potential. The shapes of the ON and OFF transients in trace 2 are somewhat different from those in trace 1, but the amounts of OFF charge in both traces are the same (see Fig. 1 *B*). After trace 2 was taken, 100 μM tetracaine was applied to the center pool. Trace 3 in Fig. 1 *A*, taken after ~10 min, has a less pronounced I_γ hump and a diminished OFF charge (Fig. 1 *B*) compared with the control. Two other traces were taken at the same concentration of tetracaine. Although traces 4 and 5 have almost the same amount of OFF charge as trace 3, the I_γ hump in trace 5 appears to have a broader time course than that in trace 3. After the concentration of tetracaine was increased to 500 μM, traces 6 and 7 were taken. The amount of OFF charge is decreased further to $<50\%$ of the control value by this higher concentration of tetracaine and no I_γ hump can be visualized in the ON segments. In trace 7, the amount of ON charge appears to be less than the amount of OFF charge. This is probably due to a progressive broadening of the time course of some residual I_γ buried in the baseline of the ON segment. We have noted previously that, when the I_γ kinetics is slow in the intermediate potential range, the amount of ON charge cannot be estimated reliably (Figs. 11 and 12 of Hui and Chandler, 1991).

These results show that, in cut fibers, submillimolar concentrations of tetracaine clearly suppress charge movement, particularly the Q_γ component, in agreement with the finding of Vergara and Caputo (1983). Although the OFF charge is presented as the amount of charge divided by the membrane capacitance measured between -110 and -90 mV, $c_m(-100)$, the reduction in OFF charge in the presence of tetracaine was not due to an increase in the membrane capacitance. In fact, $c_m(-100)$ in this fiber was reduced somewhat after the application of tetracaine.

The pharmacological effects revealed by Fig. 1 could be due to a real suppression of the amount of moveable charge. On the other hand, since charge movement was monitored at a fixed potential, the apparent suppression could be due to a shift of

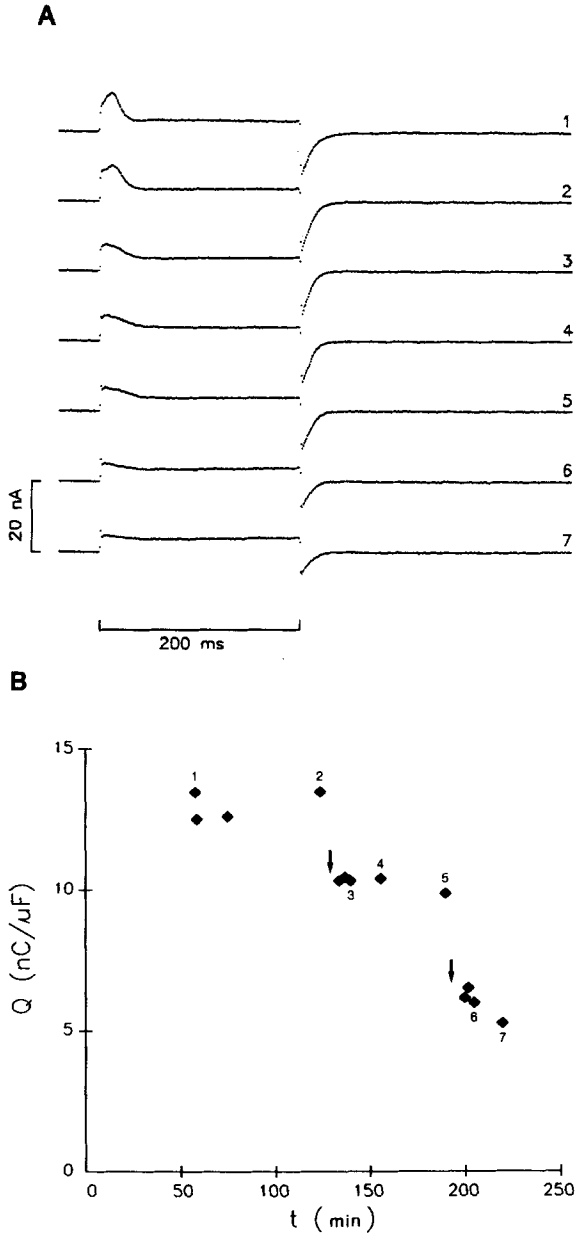

FIGURE 1. Effect of tetracaine on charge movement in a cut fiber. Fiber identification: 80061. Diameter = 102 μm. Sarcomere length = 3.5 μm. Saponin treatment was applied to membrane segments in both end pools at time zero. After rinsing, the solutions in the end pools were replaced by solution B. The solution in the center pool was then changed to an isotonic TEA.Cl solution (solution C). At the 26th minute the voltage clamp was turned on and the holding potential was set at −90 mV. From the beginning to the end of the experiment, the holding current changed from −24 to −31 nA and $r_e/(r_e + r_i)$ remained unchanged at 0.989. (*A*) TEST-minus-CONTROL current traces elicited by a TEST pulse to −45 mV. They correspond to the points marked by the respective numbers in *B*. (*B*) OFF charges estimated from TEST-minus-CONTROL current traces and plotted as a function of time. The first arrow indicates the application of 0.1 mM tetracaine to the external solution, whereas the second arrow indicates the increase of tetracaine concentration to 0.5 mM. Many traces were taken at other potentials but the values of OFF charge are not included in the plot.

the steady-state voltage distribution of charge (i.e., *Q-V* plot) in the depolarizing direction. The experiments in the following sections were carried out to determine which possibility is true. In addition, a small part of the suppression could be due to fiber rundown, but it is unlikely that all the suppression was caused by fiber rundown (see below).

Effect of a Low Concentration of Tetracaine on Charge Movement

Fig. 2 *A* shows a family of TEST-minus-CONTROL current traces elicited by TEST pulses to potentials ranging from −80 to −10 mV. These traces, taken before the application of tetracaine, resemble those recorded under identical conditions (Hui

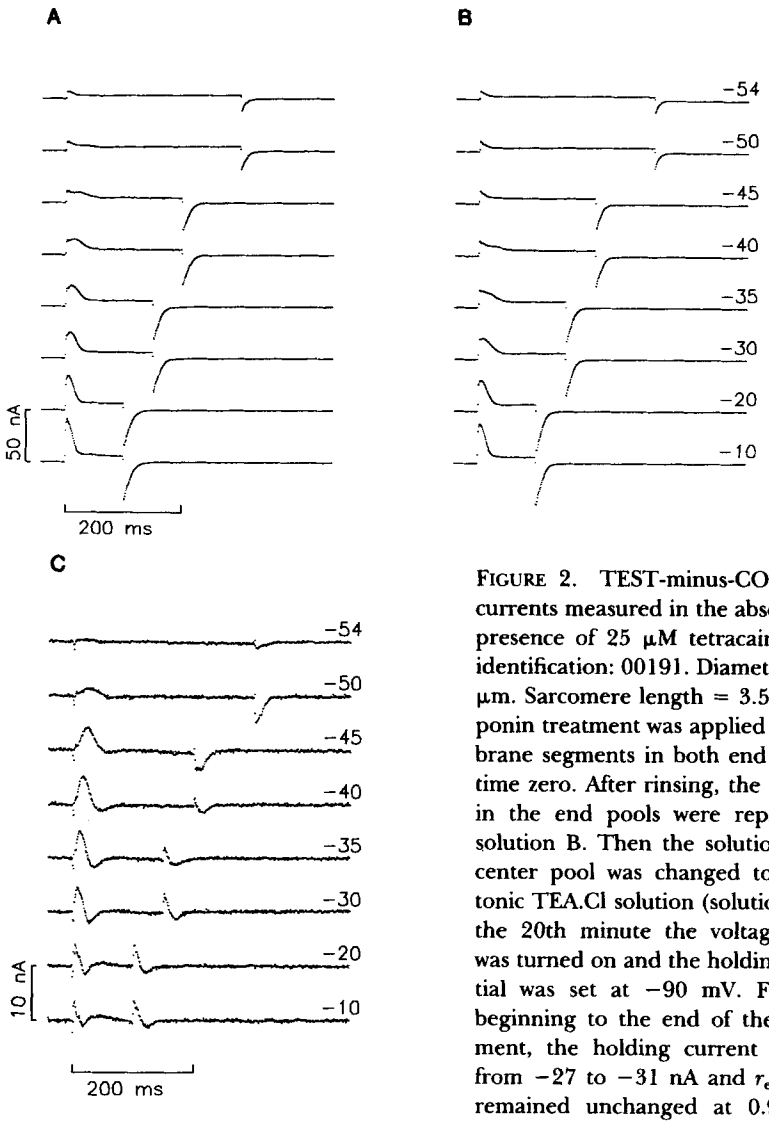

FIGURE 2. TEST-minus-CONTROL currents measured in the absence and presence of 25 μM tetracaine. Fiber identification: 00191. Diameter = 126 μm. Sarcomere length = 3.5 μm. Saponin treatment was applied to membrane segments in both end pools at time zero. After rinsing, the solutions in the end pools were replaced by solution B. Then the solution in the center pool was changed to an isotonic TEA.Cl solution (solution C). At the 20th minute the voltage clamp was turned on and the holding potential was set at −90 mV. From the beginning to the end of the experiment, the holding current changed from −27 to −31 nA and $r_e/(r_e + r_i)$ remained unchanged at 0.991. (*A*) Traces taken from the 54th to the 74th minute. At the 81st minute 25 μM tetracaine was added to the external solution. (*B*) Traces taken from the 101st to the 121st minute. The numbers at the right show the potentials during the TEST pulses (the same for the traces in *A* and *B*). (*C*) Difference traces obtained by subtracting each trace in *B* from the trace in the same row in *A*. Only representative traces are shown in each panel.

and Chandler, 1990). At potentials ≤ -54 mV, only fast transients, presumably I_β, can be seen in the ON and OFF segments of the traces. At -50 mV, a small and broad I_γ hump begins to appear in the decay phase of the I_β component in the ON segment, but not in the OFF segment. At -45 mV, the I_γ hump becomes more prominent. With further depolarizations, the peak amplitude of the I_γ hump increases progressively and actually rises above the peak of the I_β component, whereas its kinetics becomes faster such that, at the strongest depolarizations, it merges with the early I_β component and the two components cannot be visually resolved.

The traces in Fig. 2 *B* were taken after the application of 25 μM tetracaine. The I_γ humps in the ON segments at -50 and -45 mV disappear, whereas those at -40 to -30 mV are suppressed and their time courses are prolonged. The amplitudes of the OFF transients at -50 and -45 mV also appear to be suppressed.

To examine more closely the changes in waveforms of the ON and OFF transients due to the presence of this low concentration of tetracaine, the traces in Fig. 2 *B* were subtracted from the corresponding traces in Fig. 2 *A* and the difference traces are shown in Fig. 2 *C*. At -50 mV, the ON transient is bell-shaped and the OFF transient decays monotonically. The area of the OFF transient amounts to 3.1 nC/μF. At -45 mV, the bell-shaped ON transient increases in magnitude but is followed by a small undershoot. The OFF transient also has a broader peak than that in the trace above and the area of the OFF transient amounts to 3.4 nC/μF. The biphasic appearance of the ON transient in the difference trace was probably caused by a broadening of the waveform of the I_γ hump in Fig. 2 *B* by tetracaine. With larger depolarizations, the biphasic appearance is enhanced until, at -10 mV, the late negative phase is almost as large as the early positive phase. Interestingly, the time courses of the OFF transients in the current traces of Fig. 2 *B* were shortened by tetracaine such that, at potentials ≥ -40 mV, the OFF transients in the difference traces of Fig. 2 *C* show a positive phase preceding a negative phase. The net amount of OFF charge in the difference trace at -10 mV is practically zero, suggesting that there is no reduction of OFF charge in the TEST-minus-CONTROL current traces at large depolarizations in the presence of 25 μM tetracaine.

One way to quantitate the effects of 25 μM tetracaine on Q_β and Q_γ is to separate the steady-state *Q-V* plots in the absence and in the presence of tetracaine by fitting each plot with a sum of two Boltzmann distribution functions (Hui and Chandler, 1990). Since the CONTROL pulse was applied from -110 to -90 mV, a scaled amount of the CONTROL charge was subtracted from each TEST charge. This can be corrected by subtracting a straight line, which intersects the original curve at -110 and -90 mV, from the curve, similar to the procedure used by Melzer et al. (1986). The amount of charge Q is then related to the potential V by:

$$Q(V) = \sum_{i=\beta}^{\gamma} Q_{i,\max} F_i^*(V) \tag{1}$$

in which $Q_{i,\max}$ represents the maximum amount of charge for $i = \beta$ or γ, and each (normalized) modified Boltzmann distribution function is defined by:

$$F_i^*(V) = F_i(V) - [F_i(-90) - F_i(-110)](V + 110)/20 - F_i(-110) \tag{2}$$

$$F_i(V) = \left[1 + \exp\left(-\frac{V - \overline{V}_i}{k_i}\right)\right]^{-1} \quad (3)$$

in which $\overline{V}_i$ represents the equi-distribution potential and k_i the voltage dependence (or inverse steepness) factor for $i = \beta$ or γ. This procedure will be referred to as CONTROL charge correction. The component with a larger value of k can be identified with Q_β and that with a smaller value with Q_γ (see below and Hui, 1991*a*). Hui and Chandler (1990) found that the fit with a sum of two Boltzmann distribution functions was invariably better than that with a single Boltzmann distribution function and the improvement in the quality of fit was statistically significant. The same improvement was confirmed in every experiment in this study.

In addition, since the Vaseline seals do not have infinite resistance, charge movement in the membranes underneath the seals contribute to the total charge. This can be corrected for by the method of Hui and Chandler (1990), which will be referred to as gap correction.

Fig. 3 *A* shows two superimposed plots of OFF charge, estimated from the traces in Fig. 2, *A* and *B*, and other traces not shown, as a function of TEST pulse potential. The two plots have essentially identical magnitudes and shapes, except that the plot in the presence of 25 μM tetracaine is shifted a few millivolts to the right. Curves 1 and 2 were obtained by least-squares fitting Eq. 1, with gap correction, to the two sets of data. Curve 1, representing the control, intersects the voltage axis at −110 and −90 mV and dips below the axis in between as a result of CONTROL charge correction. At > −90 mV it rises above the axis with a shallow foot. Between ~ −55 and ~ −45 mV it rises steeply due to the strongly voltage-dependent activation of Q_γ. The top portion of the curve rises with a shallow slope due to the additional activation of Q_β, which is weakly voltage dependent. The value of the maximum total charge, i.e., $q_{\beta,max}/c_m + q_{\gamma,max}/c_m$ listed in the figure legend, is 24.8 nC/μF.

Curve 2 in Fig. 3 *A* shows the *Q-V* distribution in the presence of 25 μM tetracaine. The maximum amount of total charge in curve 2 is practically identical to that in curve 1. From the values of $q_{\beta,max}/c_m$ and $q_{\gamma,max}/c_m$ in the figure legend, it appears that 25 μM tetracaine had no significant effect on the amount of Q_β or Q_γ, in agreement with the finding of Csernoch et al. (1988). However, if the amounts of charge in the presence of tetracaine (open squares in Fig. 3 *A*) are subtracted pairwise from the control amounts (filled diamonds in Fig. 3 *A*), the difference plot (filled diamonds in Fig. 3 *B*) is bell-shaped, with a peak value of ~ 5 nC/μF at ~ −48 mV. The smooth curve in Fig. 3 *B* was obtained by subtracting curve 2 in Fig. 3 *A* from curve 1. The bell shape of the curve arose from a shift of the *Q-V* distribution to the right by tetracaine ($\overline{V}_\gamma$ of curve 2 is 4 mV less negative than that of curve 1).

In the two-state Boltzmann model with first order kinetics, a voltage shift of the steady-state distribution of a charge component is accompanied by a parallel voltage shift of the kinetics of the charge component (Chandler et al., 1976*a*). This explains readily the complicated kinetics of the ON and OFF transients in the difference traces of Fig. 2 *C*. The shift in $\overline{V}_\gamma$ provided a net ON or OFF charge in the difference traces at ~ 10 mV below to ~ 10 mV above −48 mV. Beyond this potential range, there should be no net ON or OFF charge in the difference traces, but the mismatch

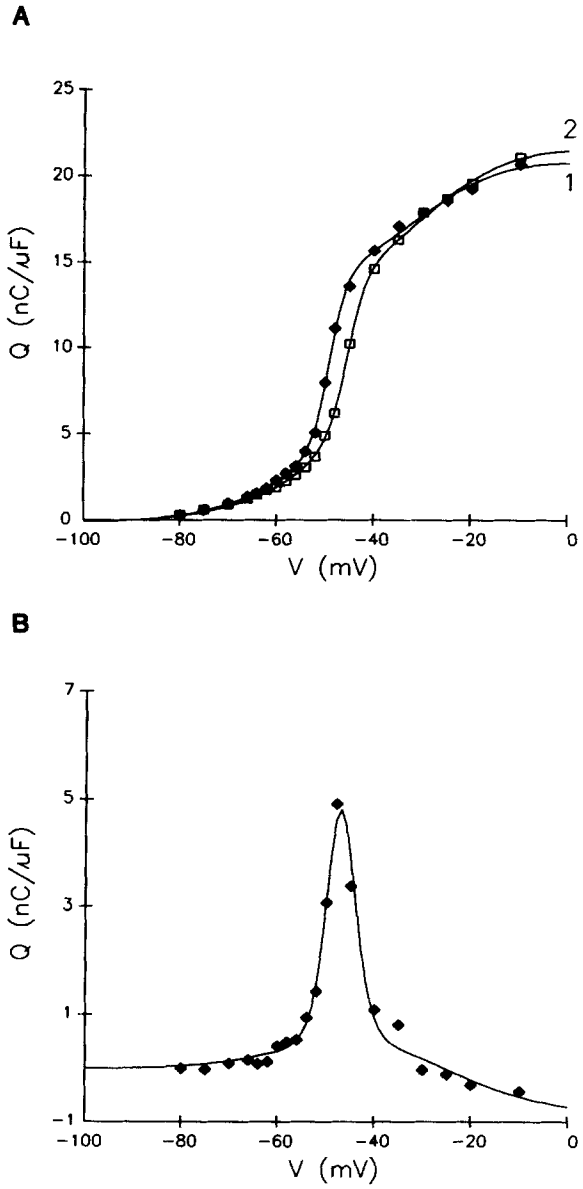

FIGURE 3. Steady-state voltage distributions of total charge in the absence and presence of 25 μM tetracaine. Same fiber as in Fig. 2. (*A*) Points obtained from time integrals of OFF transients in TEST-minus-CONTROL current traces, some of which are shown in Fig. 2, *A* and *B*. ◆'s and □'s show data taken without and with tetracaine. Curves 1 and 2 were obtained by fitting Eq. 1, with gap correction, to each set of data. The best fit parameters are:

Curve	$q_{\beta,max}/c_m$	$\overline{V}_\beta$	k_β	$q_{\gamma,max}/c_m$	$\overline{V}_\gamma$	k_γ
	nC/μF	*mV*	*mV*	*nC/μF*	*mV*	*mV*
1	11.6	−32.9	10.9	13.2	−49.9	1.7
2	12.3	−31.1	10.5	12.3	−46.1	1.9

(*B*) Difference plot obtained by subtracting each □ in *A* from the corresponding ◆. The smooth curve was obtained from the difference of curves 1 and 2 in *A*.

of the ON kinetics before and after the application of tetracaine gave a biphasic appearance to the ON transients in the difference traces. This explains some of the effects of tetracaine observed by Csernoch et al. (1989).

Five other experiments were performed with 25 μM tetracaine. On average, Q_β and Q_γ were changed to 91.0% (SEM 5.6) and 101.3% (SEM 2.4) of control, respectively (Table I), and $\overline{V}_\gamma$ was shifted 3.7 (SEM 0.7) mV in the depolarizing direction. Although the magnitude of the shift was small, it was always positive in all our experiments in this group and was sufficient to provide an obvious bell shape in every difference *Q-V* curve.

Effect of a High Concentration of Tetracaine on Charge Movement

Fig. 4 shows an experiment carried out with a higher concentration of tetracaine. The control traces shown in panel *A* are similar to those in Fig. 2 *A* with equally prominent I_γ humps, except that the threshold for Q_γ in Fig. 4 *A* appears to be ~10

TABLE I

Effects of Different Concentrations of Tetracaine on Q_β and Q_γ

	(1)	(2)	(3)	(4)	(5)	(6)	(7)	(8)	(9)	(10)	(11)	(12)
	% of Q_β remaining						% of Q_γ remaining					
	0.025	0.05	0.1	0.2	0.5	1.0	0.025	0.05	0.1	0.2	0.5	1.0
With gap correction												
Mean	91.0	97.8	70.8	96.2	98.1	98.2	101.3	93.6	79.3	74.4	32.8	0
SEM	5.6	9.1	5.5	7.6	9.9	12.7	2.4	3.9	8.3	6.3	7.1	—
Without gap correction												
Mean	105.4	112.5	112.3	101.6	93.0	76.7	102.0	97.4	67.3	81.9	33.3	0
SEM	4.1	5.1	4.5	2.6	7.6	4.0	4.6	5.4	7.8	7.3	6.4	—
n	6	6	7	8	11	5	6	6	7	8	11	5

The Q_β and Q_γ components of each *Q–V* plot were separated by fitting the plot with a sum of two Boltzmann distribution functions, with CONTROL charge correction and with or without gap correction. The percentage of Q_β and Q_γ remaining after the addition of a certain concentration of tetracaine (shown in millivolts in the heading) was calculated from the ratio of the value of $q_{i,max}/c_m$ ($i = \beta$ or γ) in the presence of the drug to the control value. The mean percentages for Q_β are listed in columns 1–6 and those for Q_γ in columns 7–12, with the SEMs below. The last row shows the numbers of fibers. Fiber diameters, 76–126 μm.

mV lower than that in Fig. 2 *A*. After the control traces were recorded, the fiber was exposed to 0.5 mM tetracaine and many traces (not shown) were taken. The current transients in those traces were markedly suppressed. On increasing the concentration of tetracaine from 0.5 to 1 mM, the current transients were further suppressed (Fig. 4 *B*). Since there is absolutely no sign of any I_γ hump at all potentials, the residual current transients in the presence of 1 mM tetracaine are assumed to be predominantly, or purely, I_β currents. As the OFF transients in the traces of Fig. 4 *A* consist of both I_β and I_γ currents, the slower time courses of the OFF transients in Fig. 4 *A*, compared with those in Fig. 4 *B*, support the finding that the OFF kinetics of I_β is faster than that of I_γ at −90 mV (Hui and Chandler, 1991).

The difference traces obtained by pairwise subtractions of the traces in Fig. 4, *A*

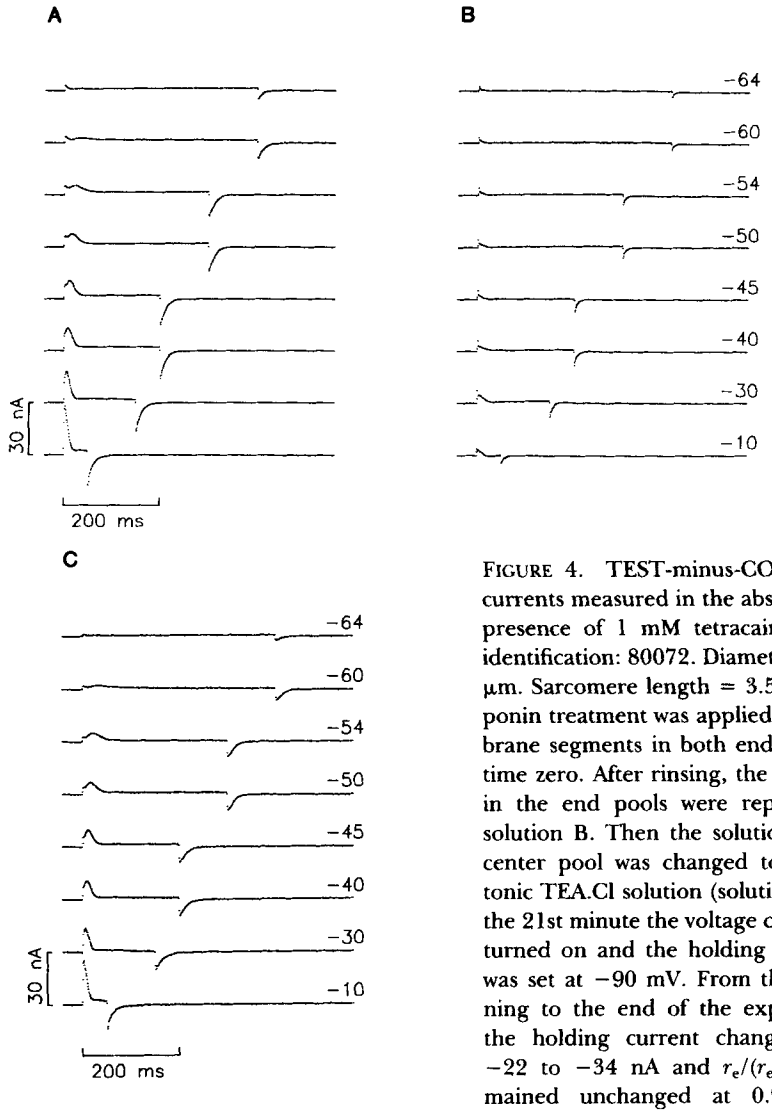

FIGURE 4. TEST-minus-CONTROL currents measured in the absence and presence of 1 mM tetracaine. Fiber identification: 80072. Diameter = 113 μm. Sarcomere length = 3.5 μm. Saponin treatment was applied to membrane segments in both end pools at time zero. After rinsing, the solutions in the end pools were replaced by solution B. Then the solution in the center pool was changed to an isotonic TEA.Cl solution (solution C). At the 21st minute the voltage clamp was turned on and the holding potential was set at −90 mV. From the beginning to the end of the experiment, the holding current changed from −22 to −34 nA and $r_e/(r_e + r_i)$ remained unchanged at 0.992. (*A*) Traces taken from the 55th to the 75th minute. At the 104th minute 0.5 mM tetracaine was added to the external solution. Many traces (not shown) were taken. At the 171st minute the concentration of tetracaine in the external solution was changed to 1 mM. (*B*) Traces taken from the 191st to the 211st minute. The numbers at the right show the potentials during the TEST pulses (the same for the traces in *A* and *B*). (*C*) Difference traces obtained by subtracting each trace in *B* from the trace in the same row in *A*. Only representative traces are shown in each panel.

and *B* are shown in Fig. 4 *C*. The current transients in these difference traces should contain primarily I_γ currents. Indeed, the ON transients are monophasic and bell-shaped, very different from the difference traces of Fig. 2 *C*. The OFF transients decay monotonically and have slower kinetics than those in Fig. 4 *B*. The ON

transients between −60 and −45 mV, perhaps even −40 mV, show a small shoulder in the rising phase, suggesting that I_β might have been affected slightly by 1 mM tetracaine.

The amounts of OFF charge from the traces in Fig. 4, *A* and *B*, and other traces not shown, are plotted against TEST pulse potential in Fig. 5. Curve 1 was obtained by least-squares fitting Eq. 1, with gap correction, to the filled diamonds. Again, this curve represents the control and resembles curve 1 in Fig. 3 *A*, except that curve 1 in Fig. 5 *A* is shifted ~10 mV to the left as compared with that in Fig. 3 *A*.

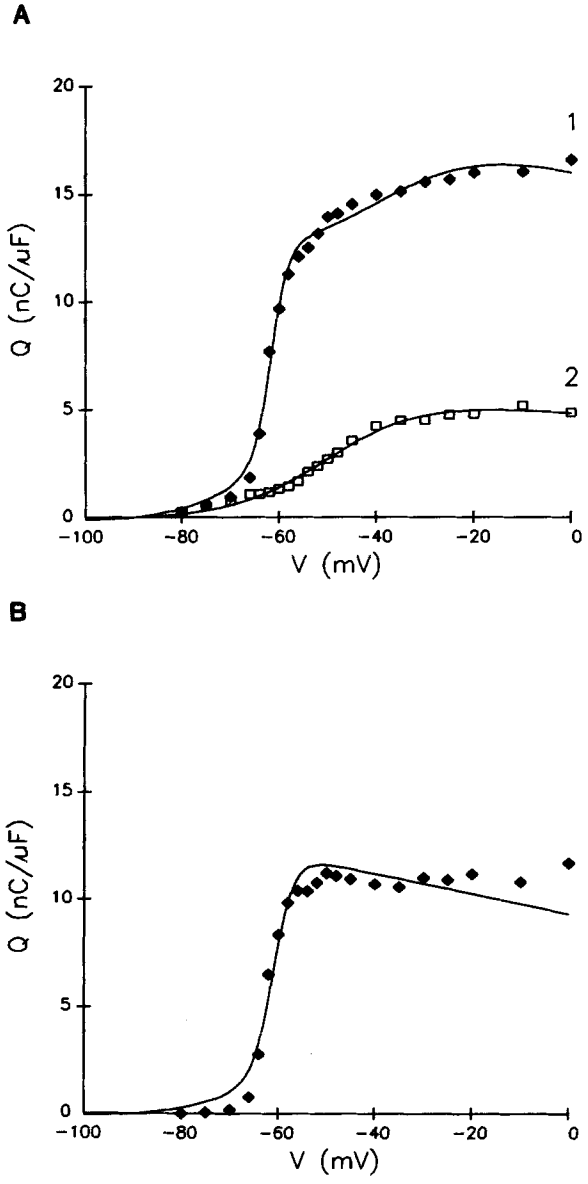

FIGURE 5. Steady-state voltage distributions of total charge in the absence and presence of 1 mM tetracaine. Same fiber as in Fig. 4. (*A*) Points obtained from time integrals of OFF transients in TEST-minus-CONTROL current traces, some of which are shown in Fig. 4, *A* and *B*. ◆'s and □'s show data taken without and with tetracaine. Curve 1 was obtained by fitting Eq. 1, with gap correction, to the ◆'s. The best fit parameters are: $q_{\beta,max}/c_m$ = 8.7 nC/μF, $\overline{V}_\beta$ = −39.6 mV, k_β = 11.2 mV, $q_{\gamma,max}/c_m$ = 14.0 nC/μF, $\overline{V}_\gamma$ = −62.4 mV, and k_γ = 1.8 mV. Curve 2 was obtained by fitting a single Boltzmann distribution function, with CONTROL charge correction and gap correction, to the □'s. The best fit parameters are: q_{max}/c_m = 6.6 nC/μF, $\overline{V}$ = −49.6 mV, and k = 9.5 mV. (*B*) Difference plot obtained by subtracting each □ in *A* from the corresponding ◆. The smooth curve was obtained by fitting a single Boltzmann distribution function, with CONTROL charge correction and gap correction, to the points. The best fit parameters are listed in the sixth row of Table II.

In the presence of 1 mM tetracaine, the maximum amount of total charge was greatly suppressed (open squares in Fig. 5 *A*). When the *Q-V* plot was fitted by Eq. 1, with or without gap correction, the fitting routine did not converge. However, the plot was fitted well by a single Boltzmann distribution function (curve 2), with CONTROL charge correction and gap correction. This suggests that probably only one charge component remained mobile in the presence of this high concentration of tetracaine. Since no I_γ humps can be visualized in the traces of Fig. 4 *B*, it is reasonable to assume that the residual charge in curve 2 is Q_β. The k value of 9.5 mV obtained from the fit supports this idea. Under this assumption, the residual amounts of Q_β and Q_γ were 75.5 and 0% of control, respectively. Thus, in this fiber, 1 mM tetracaine completely suppressed Q_γ. Unexpectedly, it also suppressed Q_β partially.

TABLE II

Steady-State Voltage Distributions of Q_γ Separated by Tetracaine (Method 1)

(1) Fiber reference	(2) [Tetracaine]	(3) $c_m(-100)$ Control	(4) $c_m(-100)$ Test	(5) $\overline{V}_\gamma$	(6) k_γ	(7) $q_{\gamma,max}/c_m$
	mM	*μF/cm*	*μF/cm*	*mV*	*mV*	*nC/μF*
88101	0.5	0.212	0.215	−54.5	3.5	5.4
88241	0.5	0.121	0.122	−56.0	1.3	5.1
89221	1	0.215	0.213	−55.8	4.1	10.2
89231	1	0.163	0.158	−54.1	1.4	8.6
89271	1	0.153	0.153	−57.5	2.3	11.4
80072	1	0.175	0.179	−61.8	2.1	14.5
Mean				−56.6	2.5	9.2
SEM				1.1	0.5	1.5

Columns 1 and 2 give the fiber identifications and the concentrations of tetracaine in the external solution. Columns 3 and 4 give the values of c_m, measured between −110 and −90 mV, in the absence and presence of tetracaine. The amount of charge blocked by tetracaine was obtained from the difference of the charge before and after the application of the drug and plotted against the TEST pulse potential. The difference *Q–V* plot, similar to that shown Fig. 5 *B*, was fitted by a Boltzmann distribution function, with CONTROL charge correction and gap correction. The best fit parameters are listed in columns 5–7. Fiber diameters, 79–113 μm.

However, this effect was not observed in all the fibers to which 1 mM tetracaine was applied (see below).

The differences between the filled diamonds and open squares in Fig. 5 *A* are shown in Fig. 5 *B*. The data can be fitted moderately well by a single Boltzmann distribution function (smooth curve), with CONTROL charge correction and gap correction. The upper part of the fitted curve has a negative slope, which arises as a result of CONTROL charge correction (Hui and Chandler, 1990). The data points > -30 mV are above the theoretical curve, probably due to the portion of Q_β suppressed by the high concentration of tetracaine. In any case, the sigmoidicity of the charge suppressed by tetracaine and its steep voltage dependence are shown convincingly in Fig. 5 *B*. The best fit parameters of the Boltzmann distribution function are listed in the sixth row of Table II. These numbers are very close to the

values of the parameters for the Q_γ component in curve 1 of Fig. 5 *A* (see figure legend). Thus, the identification of the tetracaine-sensitive charge separated by method 1 with the Q_γ charge separated by method 3 is justified.

Effect of an Intermediate Concentration of Tetracaine on Charge Movement

When a submaximal concentration (< 1 mM) of tetracaine is used, its effect on Q_γ is a combination of the two effects described in preceding sections; namely, the amount of Q_γ is partially suppressed and the Q-V plot of the residual Q_γ is shifted in the depolarizing direction, as illustrated by the experiment shown in Fig. 6. This fiber had the largest residual fraction of Q_γ in 0.5 mM tetracaine and is chosen to emphasize the complication. Curves 1 and 2 represent the best fits of Eq. 1 to the Q-V plots of OFF charge before and after the application of 0.5 mM tetracaine (data not shown). Filled diamonds, obtained by pairwise subtractions of the amounts of OFF charge before and after the application of tetracaine, represent the amounts of OFF charge blocked by the drug. They are fitted well by curve 3, which was obtained by subtracting curve 2 from curve 1. The complicated shape of curve 3 is the consequence of a partial suppression of Q_γ (and apparently also of Q_β) plus a shift of the residual Q_γ-V curve to the right. It is equivalent to superimposing the bell-shaped difference curve in Fig. 3 *B*, resulting from a pure shift of the Q_γ-V curve, on the sigmoidal difference curve in Fig. 5 *B*, resulting from a complete suppression of the Q_γ-V curve.

Fig. 6 *B* shows that the hump in curve 3 of Fig. 6 *A* can be eliminated by artificially abolishing the shift of the Q_γ-V curve. Curve 1 in Fig. 6 *B* is replotted from that in Fig. 6 *A*. Curve 2 in Fig. 6 *A* was modified by changing the value of $\overline{V}_\gamma$ to match that in curve 1 and is shown as curve 2 in Fig. 6 *B*. In this case, the difference of curves 1 and 2 in Fig. 6 *B*, represented by curve 3, does not have a hump. Thus, even when a submaximal concentration of tetracaine is used, as long as the Q_γ-V curve is not shifted, the difference curve has a sigmoidal shape. An example for this will be shown in Fig. 10 *B*. A better way to ensure obtaining a sigmoidal difference curve is to use, whenever possible, a full concentration (1 mM) of tetracaine that leaves no, or very little, residual Q_γ.

Dose–Response Relationships of the Blockages of Q_β and Q_γ by Tetracaine

The residual fractions of Q_β and Q_γ from 26 cut fibres in the presence of different concentrations of tetracaine are pooled together in Table I. All the concentrations of tetracaine were not always applied to each fiber. In the experiments in which more than one concentration was used, the concentrations were always applied in an increasing order. The mean values in the first row show that all concentrations, except 0.1 mM, of tetracaine have no effect on Q_β, in agreement with the finding of Almers and Best (1976), but suppress Q_γ in a dose-dependent manner. 1 mM tetracaine is capable of suppressing Q_γ completely. Even 0.5 mM tetracaine can sometimes suppress Q_γ completely or otherwise suppress a great fraction of Q_γ, similar to the observations of Vergara and Caputo (1983) in cut fibers but different from the findings of Huang (1982) and Hui (1983*a*) in intact fibers. In the latter preparation, a concentration of 2–4 mM is required to accomplish the effect of 0.5–1 mM in cut fibers.

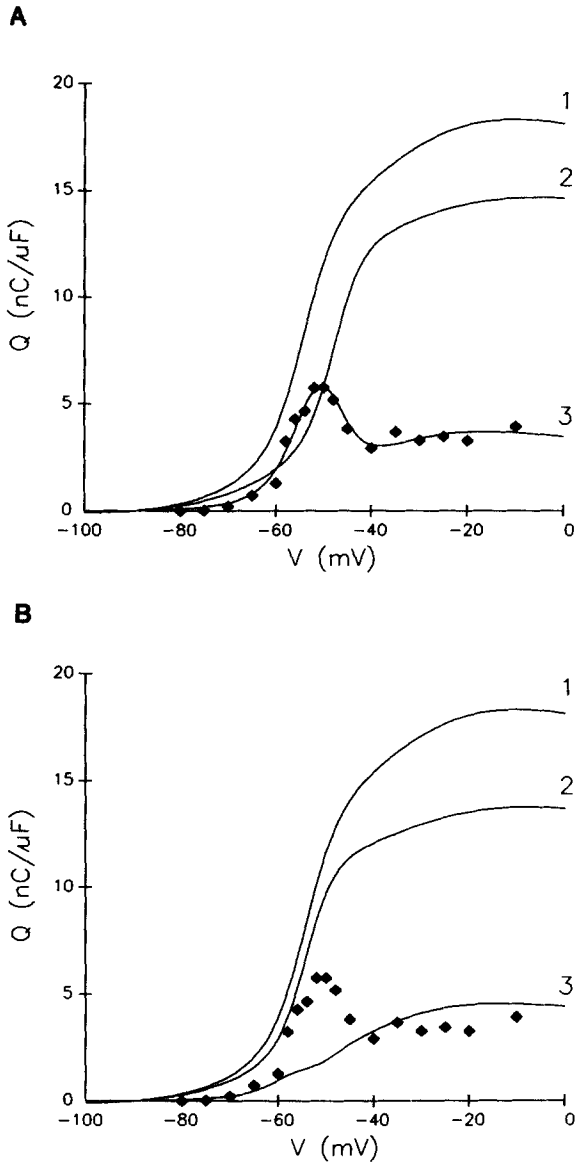

FIGURE 6. Effect of 0.5 mM tetracaine on the steady-state voltage distribution of total charge. Fiber identification: 87191. Diameter = 102 μm. Sarcomere length = 3.5 μm. Saponin treatment was applied to membrane segments in both end pools at time zero. After rinsing, the solutions in the end pools were replaced by solution B. Then the solution in the center pool was changed to an isotonic TEA.Cl solution (solution C). At the 29th minute the voltage clamp was turned on and the holding potential was set at −90 mV. From the beginning to the end of the experiment, the holding current changed from −40 to −50 nA and $r_e/(r_e + r_i)$ decreased from 0.986 to 0.982. (*A*) Control data (not shown) were taken from the 66th to the 86th minute. At the 91st minute 0.5 mM tetracaine was added to the external solution. Test data (not shown)

Other than the experiment shown in Figs. 4 and 5, five other experiments were performed in which Q_γ was completely suppressed by tetracaine. In these experiments, the ON segments of the traces from those fibers did not show any I_γ hump, similar to the traces in Fig. 4 *B*, and the *Q-V* plots could not be fitted by Eq. 1, similar to the open squares in Fig. 5 *A*. The *Q-V* plots could be fitted well, however, by a single Boltzmann distribution function, with CONTROL charge correction and gap correction, and the best fit parameters are listed in Table II. On average, 0.5–1 mM tetracaine can dissect out 9.2 nC/μF of Q_γ from the total charge.

In view of the fact that other investigators did not fit their *Q* versus *V* data with gap correction, all the *Q-V* plots in this paper were also fitted by Eq. 1 without gap correction. For comparison, the mean residual fractions so obtained are also listed at the bottom of Table I. The values for Q_γ do not differ substantially from those obtained with gap correction, whereas the values for Q_β differ more, with the effect of 0.1 mM tetracaine most different. In principle, the fitting with gap correction should be more accurate than that without. However, there is a slight possibility that the gap correction procedure could be over-correcting the charge underneath the Vaseline seals, because a detailed kinetic correction for the current underneath the seals has not been developed. Thus, the actual fractions of Q_β and Q_γ remaining at each concentration of tetracaine could be between the two extremes given by the values in the table. Other possible sources of error in the separation procedure will be presented in the Discussion.

From the results shown in this and the preceding sections, the steeply voltage-dependent component in a control *Q-V* plot can be identified with the tetracaine-sensitive component. To suppress Q_γ completely in cut fibers, 0.5–1 mM tetracaine will be required. When a low concentration, such as 25 μM, of tetracaine is used, Q_γ is not suppressed but its activation curve is shifted a few millivolts in the depolarizing direction. As a result, one should be particularly cautious in obtaining difference current traces or differences between the amounts of charge, before and after the application of tetracaine at a single potential that lies in the steep segment of the *Q-V* curve, as such a difference might provide misleading information.

FIGURE 6 (*continued*) were taken from the 110th to the 130th minute. Curves 1 and 2 were obtained by fitting Eq. 1, with gap correction, to the control and test data sets. The best fit parameters are:

Curve	$q_{\beta,max}/c_m$	$\overline{V}_\beta$	k_β	$q_{\gamma,max}/c_m$	$\overline{V}_\gamma$	k_γ
	nC/μF	*mV*	*mV*	*nC/μF*	*mV*	*mV*
1	9.5	−38.7	10.4	13.7	−55.4	3.4
2	7.1	−38.6	13.3	11.3	−48.7	2.9

◆'s were obtained by pairwise subtractions of points at each potential with and without tetracaine. Curve 3 was obtained by subtracting curve 2 from curve 1. (*B*) The ◆'s and curve 1 are replotted from *A*. Curve 2 is plotted by replacing the value of $\overline{V}_\gamma$ of curve 2 in *A* by that of curve 1 and using the values of the other parameters of curve 2 in *A*. Curve 3 was obtained by subtracting curve 2 from curve 1.

Reversibility of the Suppression of Charge Movement by Tetracaine

One disadvantage in the use of tetracaine is the difficulty in washing out the drug completely, particularly after a relatively high dose of the drug has been applied. This is why all the investigators who observed a suppression of charge movement by tetracaine (Huang, 1982; Hui, 1983*a*; Lamb, 1986; Hollingworth et al., 1990) did not mention the reversibility of the effect. Vergara and Caputo (1983), on the other hand, specifically mentioned that the suppression of charge movement in cut fibers by >0.5 mM tetracaine is only partially reversible.

In the experiments reported in this paper, reversibility of the effect of tetracaine on charge movement was mostly observed on isolated occasions when ≤ 0.1 mM of the drug was used. For 0.5 mM, the effect was only partially reversible, in agreement with the observation of Vergara and Caputo (1983). We did not attempt to wash out the drug after 1 mM was applied. Perhaps the most complete reversibility was demonstrated by an experiment in which the OFF charge was followed by a constant TEST pulse to −45 mV, similar to that shown in Fig. 1 *B*. The average control OFF charge, from five measurements, was 15.1 nC/μF. Three doses of tetracaine were applied, namely, 0.025, 0.1, and 0.5 mM, and the average OFF charge in the presence of these concentrations of the drug was 14.7 (n = 7), 13.2 (n = 6), and 10.6 (n = 4) nC/μF, respectively. The amount of OFF charge was reduced in steps (as in Fig. 1 *B*) and remained constant until the next dose of tetracaine was applied. This suggests that the reduction in OFF charge was caused by the presence of the drug but was not due to a gradual rundown of the fiber. Subsequently, the drug was washed out and the average OFF charge recovered to 15.7 nC/μF (n = 6), the same as the control value. Finally, 0.5 mM tetracaine was applied again and the average OFF charge fell to 11.3 nC/μF (n = 5).

Effect of Tetracaine on Q_γ during a Post-Pulse to a Potential Just above the Threshold of Q_γ

Hui and Chandler (1991) reported that if charge movement is studied with the two-pulse protocol, the inward OFF transient during the post-pulse contains two components with different decay time constants. They identified the fast component with I_β and the slow component with I_γ. The potential during the post-pulse optimal for recording the I_γ component with the longest time constant is around −60 mV, a potential just above the threshold for the activation of Q_γ.

Fig. 7 shows two traces, both elicited by a TEST pulse to −40 mV followed by a post-pulse to −62 mV. Trace 1, recorded before the application of tetracaine, shows an outward ON transient consisting of an I_β component and an I_γ component fused together. During the intermediate repolarization to −62 mV, the inward OFF transient decays with a fast and a slow exponential. When a sum of two exponentials plus a sloping straight line was fitted to the points in this segment, it yielded two time constants of values 6.4 and 85 ms. The final OFF current on repolarization to −90 mV is not shown.

After the application of 1 mM tetracaine, the ON transient was greatly suppressed. Interestingly, the slow I_γ component in the OFF transient during the post-pulse completely disappeared and the segment could be fitted well by a single exponential plus a sloping straight line. The decay time constant of the remaining, presumably I_β,

transient was 9.0 ms, not much different from the decay time constant of the I_β component in the same segment in trace 1. Hence, the slow current transient during the post-pulse is also tetracaine sensitive, consistent with the idea that the slow current transient in the post-pulse segment and the hump current component in the ON segment are associated with the same species of charge.

Hui and Chandler (1991) took advantage of the slow OFF kinetics of I_γ during the post-pulse to obtain another description of the Q_γ-V curve (method 4). The pulse protocol for a typical experiment of this kind is shown in Fig. 8 *C*. TEST pulses of varying magnitudes are followed by a 100-ms post-pulse to −60 mV. Fig. 8 *A* shows a family of TEST-minus-CONTROL current traces recorded with this protocol before the application of tetracaine. Except for the first trace, which was elicited by the post-pulse alone without a TEST pulse, and the second trace, which was elicited by a TEST pulse smaller than the post-pulse, all other traces have an ON segment (at the TEST pulse potential), an intermediate OFF segment (at the post-pulse potential),

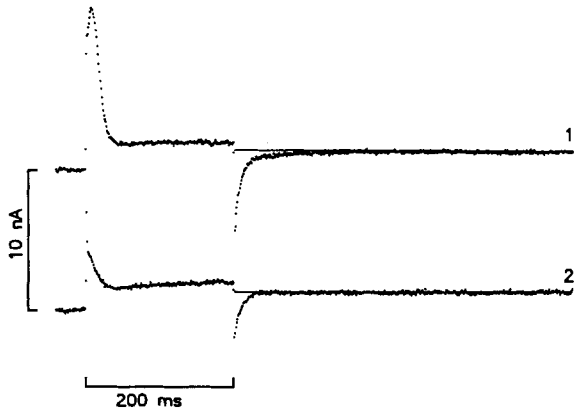

FIGURE 7. Effect of 1 mM tetracaine on TEST-minus-CONTROL current during a long post-pulse to a potential less negative than the holding potential. Same fiber as in Fig. 4. Traces 1 and 2 show the current recorded in the absence and presence of 1 mM tetracaine, respectively. Each trace shows a baseline at −90 mV preceding stimulation, then an ON segment during the TEST pulse to −40 mV, followed by an OFF segment during a post-pulse to −62 mV. The segment after the final repolarization to −90 mV is not shown. The straight line in the post-pulse segment represents the sloping baseline in the segment.

and a final OFF segment (at −90 mV). The duration of the post-pulse was chosen to be much shorter than that used in the experiment of Fig. 7. As a result, part of the slow current in the intermediate OFF segment was interrupted and was added to the final OFF current. This explains why the final OFF current in the traces of Fig. 8 *A* increases with the TEST pulse potential.

The amounts of the final OFF charge from the traces in Fig. 8 *A*, and other traces not shown, are plotted as a function of TEST pulse potential in Fig. 9 as filled diamonds. Assuming that the time constant of the slow component in the intermediate OFF segment is independent of the potential during the TEST pulse (Hui and Chandler, 1991), the final OFF charge Q at each TEST potential V can be expressed as:

$$Q(V) = A + \rho Q_{\gamma,\max}\left[1 + \exp\left(-\frac{V - \overline{V}_\gamma}{k_\gamma}\right)\right]^{-1} \quad (4)$$

in which A is a constant equal to the amount of charge moved between −60 and −90 mV and ρ is another constant equal to the fraction of Q_γ unable to return to the resting state because of the short duration of the post-pulse. If the OFF time constant of I_γ (τ_γ in milliseconds) at −60 mV is known, ρ can be calculated from the expression

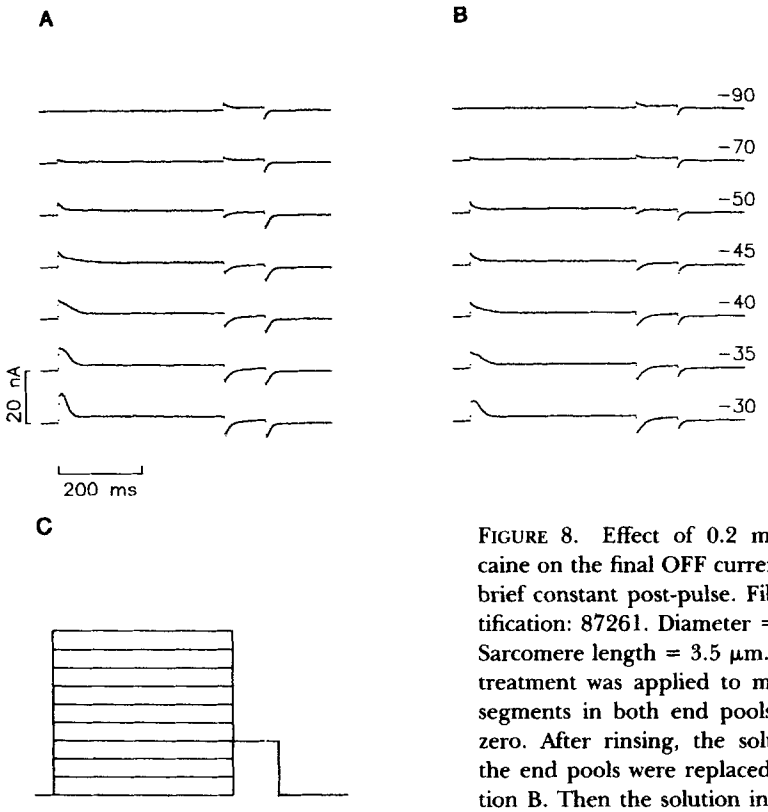

FIGURE 8. Effect of 0.2 mM tetracaine on the final OFF current after a brief constant post-pulse. Fiber identification: 87261. Diameter = 96 μm. Sarcomere length = 3.5 μm. Saponin treatment was applied to membrane segments in both end pools at time zero. After rinsing, the solutions in the end pools were replaced by solution B. Then the solution in the center pool was changed to an isotonic TEA.Cl solution (solution C). At the 24th minute the voltage clamp was turned on and the holding potential was set at −90 mV. From the beginning to the end of the experiment, the holding current changed from −24 to −32 nA and $r_e/(r_e + r_i)$ decreased from 0.990 to 0.988. Each TEST-minus-CONTROL current trace was elicited by a TEST pulse to a varying potential and a post-pulse to −60 mV lasting 100 ms, or by the post-pulse alone. (*A*) Traces taken from the 80th to the 102nd minute. At the 108th minute 0.2 mM tetracaine was added to the external solution. (*B*) Traces taken from the 161st to the 183rd minute. The numbers at the right show the potentials during the TEST pulses (same for the traces in *A* and *B*). Only representative traces are shown in each panel. (*C*) Pulse protocol. The post-pulse potential was −60 mV.

$\exp(-100/\tau_\gamma)$. Thus, a larger τ_γ gives a larger ρ. Curve 1 in Fig. 9 was obtained by fitting Eq. 4, with gap correction, to the filled diamonds. The good quality of fit suggests that the Q-V curve for the final OFF charge indeed contains a constant component plus a steep sigmoidal component. The latter component is ρ times the

Q_γ-V curve that could be separated from the Q-V curve of the total charge obtained with the one-pulse protocol.

The TEST-minus-CONTROL current traces shown in Fig. 8 *B* were taken after the application of 0.2 mM tetracaine. The current transients in the final OFF segments are noticeably reduced by the drug. The amounts of final OFF charge are plotted against TEST pulse potentials as open squares in Fig. 9. Curve 2 was obtained by fitting Eq. 4, with gap correction, to the points. A comparison of curves 1 and 2 reveals that both the constant pedestal and the amplitude of the sigmoidal component are reduced by tetracaine. This indicates that the Q_γ component separated by method 4 is also tetracaine sensitive, similar to the Q_γ component separated by method 3.

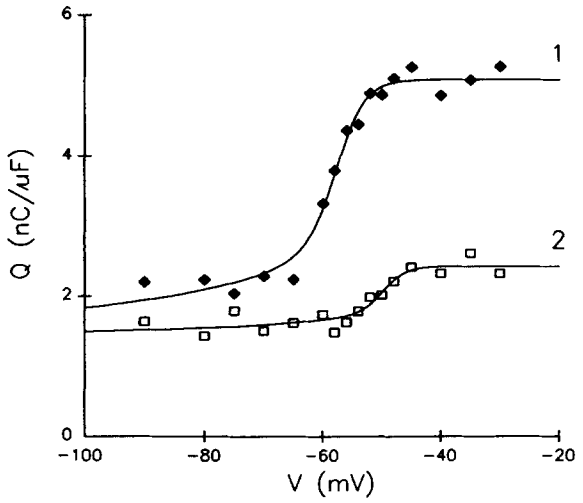

FIGURE 9. Effect of 0.2 mM tetracaine on the steady-state voltage distribution of the final OFF charge after a brief constant post-pulse. Same fiber as in Fig. 8. Points were obtained from time integrals of the final OFF currents in TEST-minus-CONTROL current traces, some of which are shown in Fig. 8, *A* and *B*. ◆'s and □'s show data taken without and with 0.2 mM tetracaine, respectively. Curves 1 and 2 were obtained by fitting Eq. 4, with gap correction, to the two data sets. The best fit parameters are:

Curve	q_{max}/c_m	$\overline{V}$	k
	nC/μF	*mV*	*mV*
1	3.3	−58.7	2.4
2	0.9	−50.6	1.9

Effects of Different Concentrations of Tetracaine on the Q_γ Components Separated by Methods 3 and 4 in the Same Fiber

The experiment shown in Figs. 10 and 11 was designed to demonstrate, in the same fiber, the tetracaine sensitivity of the Q_γ components separated by methods 3 and 4. The filled diamonds in Fig. 10 *A* show the amounts of control OFF charge plotted against TEST pulse potentials in a one-pulse protocol. With method 3, the Q_β and Q_γ components were separated by fitting curve A to the points according to Eq. 1, with gap correction. Q_γ accounts for 9.7 nC/μF, which is 63% of the total charge. In the presence of 0.1, 0.5, and 1 mM tetracaine, the amounts of OFF charge, represented in Fig. 10 *A* by open squares, filled triangles, and open inverted triangles, respectively, are suppressed in a dose-dependent manner at all potentials. One way to

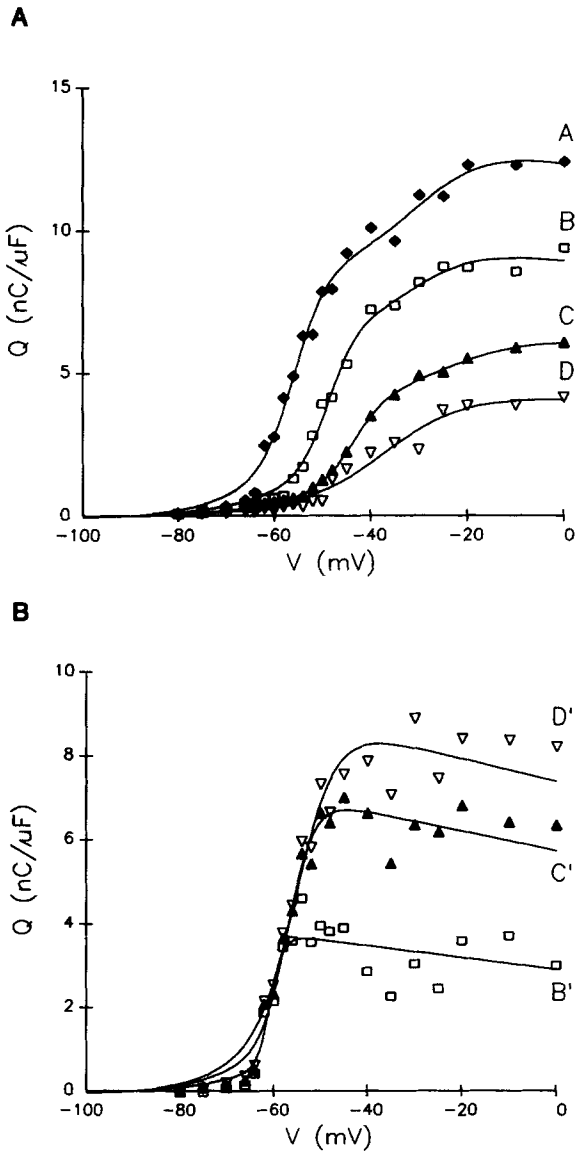

FIGURE 10. Effects of various concentrations of tetracaine on the steady-state voltage distribution of total charge. Fiber identification: 89221. Diameter = 102 μm. Sarcomere length = 3.5 μm. Saponin treatment was applied to membrane segments in both end pools at time zero. After rinsing, the solutions in the end pools were replaced by solution B. Then the solution in the center pool was changed to an isotonic TEA.Cl solution (solution C). At the 19th minute the voltage clamp was turned on and the holding potential was set at −90 mV. From the beginning to the end of the experiment, which lasted almost 6 h, the holding current changed from −24 to −59 nA and $r_e/(r_e + r_i)$ decreased from 0.990 to 0.987. (*A*) Points were obtained from time integrals of OFF currents in TEST-minus-CONTROL current traces (not shown) elicited by single TEST pulses. ◆'s were taken from the 55th to the 75th minute. At the 150th minute 0.1 mM tetracaine was added to the external solution. □'s were taken from the 165th to the 186th minute. At the 223rd minute the concentration of tetracaine was changed to 0.5 mM. ▲'s were taken from the 239th to the 259th minute. At the 292nd minute the concentration of tetracaine was changed to 1 mM. ▽'s were taken from the 304th to the 324th minute. Curves A, B, and C were obtained by fitting Eq. 1, with gap correction, and curve D was obtained by fitting a single Boltzmann distribution function, with CONTROL charge correction and gap correction, to the data sets. The best fit parameters are:

Curve	$q_{\beta,max}/c_m$	$\overline{V}_\beta$	k_β	$q_{\gamma,max}/c_m$	$\overline{V}_\gamma$	k_γ
	nC/μF	*mV*	*mV*	*nC/μF*	*mV*	*mV*
A	5.6	−30.6	7.6	9.7	−56.5	3.4
B	3.4	−31.2	6.5	7.0	−49.3	3.0
C	2.6	−24.5	8.5	4.1	−44.0	3.5

quantitate the suppressing effects of the various concentrations of tetracaine on Q_γ is to separate the *Q-V* plots in the presence of tetracaine into Q_β and Q_γ components by method 3 (curves B–D) and calculate the residual fractions of Q_γ, as was done in the experiment of Fig. 3. The results so obtained are listed in the figure legend.

Alternatively, Q_γ can be separated by method 1. Difference *Q-V* plots, similar to that in Fig. 5 *B*, are shown in Fig. 10 *B*. The open inverted triangles in Fig. 10 *B*, obtained by subtracting the open inverted triangles in Fig. 10 *A* from the corresponding filled diamonds, represent the amounts of OFF charge suppressed by 1 mM tetracaine. Curve D′ was obtained by fitting a single Boltzmann distribution function with CONTROL charge correction and gap correction. The maximum amount of charge was 10.2 nC/μF, very close to the value of $q_{\gamma,max}/c_m$ mentioned in the preceding paragraph, in agreement with the analysis associated with Fig. 5.

The sensitivity of the tetracaine-sensitive component can be studied by obtaining the difference *Q-V* plots with other lower concentrations of tetracaine. Curves C′ and B′ in Fig. 10 *B* represent the amounts of OFF charge suppressed by 0.5 and 0.1 mM tetracaine, respectively. Assuming that, in this fiber, 1 mM was the concentration of tetracaine capable of suppressing 100% of the tetracaine-sensitive component, then 0.1 and 0.5 mM tetracaine suppressed 44.1 and 80.4% of this component, respectively. These values are not exactly the same as those obtained with method 3, i.e., 28.3 and 58.0%, respectively. The slight discrepancy can be partially explained by scatter of data and partially attributed to a difference in the assumptions on which the two methods are based: in method 1 tetracaine can only affect the tetracaine-sensitive charge component, by definition, whereas in method 3 tetracaine is allowed to have an effect on both Q_β and Q_γ.

The two-pulse protocol (method 4) was also used in the same experiment and the results are shown in Fig. 11. Filled diamonds represent the amounts of final OFF charge in the absence of tetracaine. Curve 1, obtained by fitting Eq. 4, with gap correction, shows a constant pedestal and a sigmoidal component, the same as in Fig. 9. The values of $\overline{V}_\gamma$ and k_γ for the sigmoidal component, −57.0 and 3.9 mV, agree quite well with the values −56.5 and 3.4 mV obtained by method 3. On the other hand, as explained above, the amplitude of the sigmoidal component, 1.9 nC/μF, is a small fraction of 9.7 nC/μF, as expected. In the presence of 0.1 mM tetracaine, the amplitude of the sigmoidal component is reduced to 0.5 nC/μF, 27% of the control value. In the presence of 0.5 or 1 mM tetracaine, no sigmoidal component can be

FIGURE 10 (*continued*) For curve D, q_{max}/c_m = 4.4 nC/μF, $\overline{V}$ = −36.5 mV, and k = 7.9 mV. (*B*) Difference *Q-V* plots for various concentrations of tetracaine. □, ▲, and ▽ were obtained by subtracting each □, ▲, and ▽ in *A* from the corresponding ◆. Curves B′, C′, and D′ were obtained by fitting a single Boltzmann distribution function, with CONTROL charge correction and gap correction, to the three data sets. The best fit parameters are:

Curve	q_{max}/c_m	$\overline{V}$	k
	nC/μF	*mV*	*mV*
B′	4.5	−61.8	1.4
C′	8.2	−57.8	2.8
D′	10.2	−55.8	4.1

resolved. Thus, Fig. 11 clearly shows that the Q_γ component separated by method 4 can also be blocked by tetracaine in a dose-dependent manner. Because of the small fraction of Q_γ dissected out by this method, it is not worth comparing quantitatively, for this fiber, the dose–response relationship for the blockage of Q_γ estimated from the curves in Fig. 11 with that estimated by method 2.

Comparison of Q_γ Separated by the Four Methods

The second main goal of this paper is to critically compare the characteristics of the Q_γ components separated by the four different methods so as to determine whether

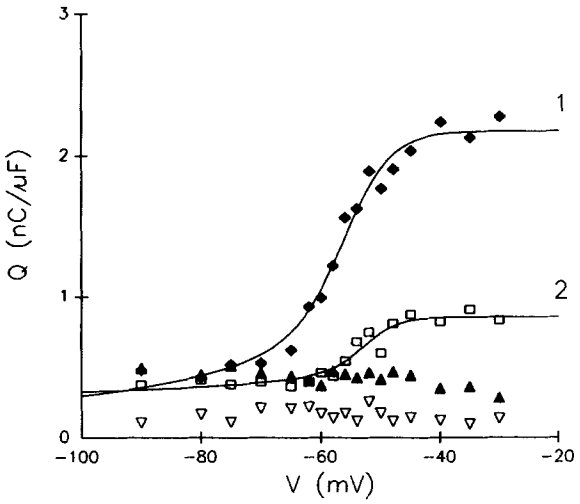

FIGURE 11. Effects of various concentrations of tetracaine on the voltage distribution of the final OFF charge after a constant brief post-pulse. Same fiber as in Fig. 10. The pulse protocol was similar to that in Fig. 8 *C*, except that the potential during the post-pulse in this experiment was −65 mV. Points were obtained from time integrals of the final OFF currents in TEST-minus-CONTROL current traces (not shown) on repolarization from −65 to −90 mV. ◆'s were taken from the 103rd to the 142nd minute. At the 150th minute 0.1 mM tetracaine was added to the external solution. □'s were taken from the 190th to the 210th minute. At the 223rd minute the concentration of tetracaine in the external solution was changed to 0.5 mM. ▲'s were taken from the 264th to the 285th minute. At the 292nd minute the concentration of tetracaine was changed to 1 mM. ▽'s were taken from the 327th to the 347th minute. Curves 1 and 2 were obtained by fitting Eq. 4, with gap correction, to the ◆'s and □'s, respectively. The best fit parameters are:

Curve	q_{max}/c_m	$\overline{V}$	k
	nC/μF	*mV*	*mV*
1	1.9	−57.0	3.9
2	0.5	−53.5	2.9

No curve was fitted to the ▲ and ▽.

the different Q_γ components can be identified with each other or whether the four sets of definitions of Q_β and Q_γ are equivalent to each other, within experimental error. The best way to accomplish this goal is to apply all four methods to the same fiber. Fig. 12 shows an experiment of this kind.

The one-pulse protocol was first applied to the fiber in the control solution. The same family of TEST-minus-CONTROL current traces (see Fig. 4 *A*) was used for separating Q_β and Q_γ by methods 2 and 3. In method 2, the current in the ON

segment of a charge movement trace was approximated by:

$$I_{ON}(t) = C_\beta \exp(-t/\tau_\beta) + C_\gamma \frac{d}{dt}\left[1 + \exp\left(-\frac{t - t_{p,\gamma}}{\tau_\gamma}\right)\right]^{-1} \quad (5)$$

The first term on the right-hand side represents I_β and is characterized by a decay time constant τ_β. The second term, representing I_γ, is the time derivative of the logistic curve (Murray, 1979) and its bell shape is characterized by its time-to-peak, $t_{p,\gamma}$, and a time constant, τ_γ. Although Eq. 5 was intended to be a phenomenological model, it might have mechanistic implication (Hui, 1991*a*). In the experiment shown in Fig. 12, only the ON segments of the traces from −62 to −45 mV were fitted by

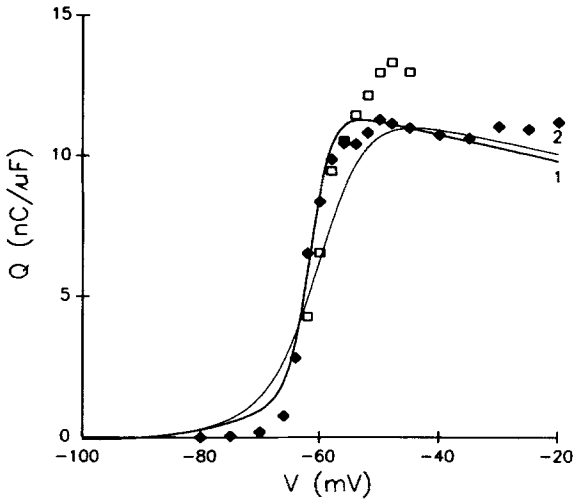

FIGURE 12. Comparison of Q_γ-V plots obtained from the same fiber using all four methods of separation. Same fiber as in Fig. 4. ◆'s represent the amounts of charge blocked by 1 mM tetracaine (method 1) and are replotted from Fig. 5 *B*. The Boltzmann parameters for the Q_γ-V curve (not shown) fitted to the ◆'s are listed in columns 5–7 of the sixth row in Table II. □'s represent the time integrals of I_γ separated by Eq. 5 (method 2). The Boltzmann parameters for the Q_γ-V curve (not shown) fitted to the □'s are: $q_{\gamma,max}/c_m$ = 16.5 nC/μF, $\overline{V}_\gamma$ = −59.8 mV, and k_γ = 3.0 mV. Curve 1 shows the Q_γ-V component separated from the Q-V plot of the total charge (◆'s in Fig. 5 *A*) by fitting Eq. 1, with gap correction (method 3). The Boltzmann parameters are: $q_{\gamma,max}/c_m$ = 14.0 nC/μF, $\overline{V}_\gamma$ = −62.4 mV, and k_γ = 1.8 mV. Curve 2 shows the Q_γ-V component obtained by fitting Eq. 4, with gap correction (method 4), to the Q-V plot of the final OFF charge after a brief constant post-pulse (data points not shown). Curve 2 is plotted with the pedestal removed. The values of $\overline{V}_\gamma$ and k_γ are −61.2 and 2.6 mV, and the value of $q_{\gamma,max}/c_m$ was adopted from that obtained with method 3.

Eq. 5 (not shown), as was done in Fig. 3 *B* of Hui (1991*a*). The time integrals of the I_γ components so obtained are plotted in Fig. 12 as open squares. The best fit parameters obtained by fitting a single Boltzmann distribution function, with CONTROL charge correction and gap correction (not shown), are listed in the figure legend.

The separation of Q_β and Q_γ for this experiment by method 3 has been shown in curve 1 of Fig. 5 *A*. The Q_γ component, described by the parameters listed in the legend of that figure, is plotted in Fig. 12 as curve 1. The two-pulse protocol was then applied in order to separate Q_γ by method 4. The Q-V plot of the final OFF charge was fitted by Eq. 4, with gap correction, as was done in Figs. 9 and 11. The sigmoidal

component so obtained is plotted in Fig. 12 as curve 2, which has been scaled to match the value of $q_{\gamma,max}/c_m$ of curve 1.

Finally, Q_γ was separated by method 1 with 1 mM tetracaine. After equilibration, the one-pulse protocol was applied. The TEST-minus-CONTROL current traces have been shown in Fig. 4 *B* and the difference *Q-V* plot in Fig. 5 *B* is replotted in Fig. 12 as filled diamonds. The best fit parameters obtained by fitting a single Boltzmann distribution function, with CONTROL charge correction and gap correction (not shown), are listed in columns 5–7 of the sixth row in Table II. A comparison of the four groups of parameters, for this fiber, shows that the four methods of separation all yield a sigmoidal charge distribution that can be fitted well by a single Boltzmann distribution function, with the maximum amount of charge lying between 14.0 and 16.5 nC/μF and $\overline{V}_\gamma$ between −59.8 and −62.4 mV. Although the values of

TABLE III

Steady-State Voltage Distributions of Q_γ Separated by a Sum of Two Kinetic Functions (Method 2), by a Sum of Two Boltzmann Distribution Functions (Method 3), and by a 100-ms Post-Pulse (Method 4)

	(1)	(2)	(3)	(4)	(5)	(6)	(7)	(8)
	Method 2			Method 3			Method 4	
	$\overline{V}_\gamma$	k_γ	$q_{\gamma,max}/c_m$	$\overline{V}_\gamma$	k_γ	$q_{\gamma,max}/c_m$	$\overline{V}_\gamma$	k_γ
	mV	*mV*	*nC/μF*	*mV*	*mV*	*nC/μF*	*mV*	*mV*
Mean	−56.8	3.9	13.5	−58.7	3.2	11.9	−59.0	2.6
SEM	0.9	0.2	0.9	1.0	0.3	0.7	1.0	0.3
n	19	19	19	19	19	19	17	17

All three methods were applied to 17 fibers, which included all six fibers listed in Table II. Only methods 2 and 3 were applied to two additional fibers. In method 2, the I_γ component at each potential was separated by fitting Eq. 5 to the ON segment of a TEST-minus-CONTROL current trace and integrated to give the amount of Q_γ. The Q_γ–*V* plot was fitted by a single Boltzmann distribution function, with CONTROL charge correction and gap correction. The best fit parameters are listed in columns 1–3. In method 3, the *Q*–*V* plot of the total charge for each fiber was fitted by a sum of two Boltzmann distribution functions, with CONTROL charge correction and gap correction. Columns 4–6 give the best fit parameters for the Q_γ component. In method 4, the *Q*–*V* plot for the final OFF charge at −90 mV was fitted by a single Boltzmann distribution function plus a constant, with gap correction. Columns 7 and 8 give the best fit parameters for the sigmoidal component. Fiber diameters, 79–124 μm.

k_γ spread from 1.8 to 3.0 mV, they are markedly smaller than the value of k_β (11.2 nC/μF as listed in the legend of Fig. 5) and support the conclusion that a steeply voltage-dependent component of charge can be separated by all four methods.

All four methods were applied to five other fibers listed in the first five rows of Table II. In 13 other experiments method 1 was not applied because no, or submaximal concentrations of, tetracaine was used. The mean values of the Boltzmann parameters obtained by the four methods, listed in Tables II and III, are in good qualitative agreement with each other, with $q_{\gamma,max}/c_m$ ranging from 9.2 to 13.5 nC/μF, $\overline{V}_\gamma$ from −59.0 to −56.6 mV, and k_γ from 2.5 to 3.9 mV. Two-tailed *t* tests were performed to evaluate the statistical significance of the differences between the corresponding values of each parameter. Instead of testing all the values pairwise, the values obtained by method 3 were taken as reference and the values obtained by

methods 1, 2, and 4 were tested against those values. Only results from the six fibers in Table II were used for comparing methods 1 and 3. Results from all 19 fibers were used for comparing methods 2 and 3, and results from the 17 fibers (columns 7 and 8 in Table III) were used for comparing methods 4 and 3. The *t* tests showed that the differences of values for each parameter are statistically insignificant ($P > 0.05$–0.8).

DISCUSSION

Strengths and Limitations of the Four Separation Methods

Method 1. This method is the most objective and does not depend on any theoretical model. Nonetheless, in identifying the tetracaine-sensitive component with Q_γ, there is an underlying assumption that tetracaine only affects Q_γ but not Q_β. This assumption may not be entirely correct because, according to method 3, tetracaine might also suppress Q_β (see Table I). Nonetheless, because of the slight uncertainties in separating Q_β and Q_γ by method 3 (see below), the minor effect of tetracaine on Q_β should not be considered unequivocal.

It seems reasonable, as in most pharmacological manipulations, to worry about the viability of the fiber upon exposure to tetracaine. In principle, a high concentration of the drug should be applied in order to block the Q_γ component completely. However, the 2–4-mM concentration that was routinely applied to intact frog fibers (Almers and Best, 1976; Huang, 1982; Hui, 1983*a*; Hollingworth et al., 1990) is absolutely damaging to cut frog fibers. Even a 0.5-mM concentration, which suppressed Q_γ incompletely in some cut fibers, caused the holding current to increase rapidly in other cut fibers. This variability in the sensitivity of the cut fibers to the drug is puzzling, but could be due to the condition of the frogs. It lowers the success rate of this kind of experiment painfully. A similar diversity in the sensitivities to tetracaine between cut and intact fibers was noticed by Lamb (1986) in mammalian muscle.

Method 2. This method conforms with the original definitions that Q_β is the early and Q_γ the hump current component in the ON segments of charge movement traces. Unfortunately, it is the most tedious and time-consuming method and can only be applied to TEST-minus-CONTROL current traces in a very narrow potential range in which the I_γ component appears as a distinct hump separable from the I_β component.

The most serious shortcoming of this method is that the exact functional form describing the time course of I_γ is unknown and the bell-shaped function used in Eq. 5 is not unique. We have repeated the separation of I_β and I_γ in all the fibers by approximating I_γ with another bell-shaped function having the same degrees of freedom. The second term in Eq. 5 was replaced by $C_\gamma \cdot d[m(t)^N]//dt$, in which $m(t) = 1 - \exp(-t/\tau_\gamma)$. Interestingly, the outcome of the separation is quite insensitive to the choice of the expression. When compared with the best fit parameters obtained by method 3, the parameters obtained by fitting Eq. 5 with the new function are still not statistically different ($P > 0.05$–0.5). A better understanding of the molecular mechanisms underlying Q_β or Q_γ will be required to determine the exact functional form describing the shape of I_γ.

Method 3. This method is based on a model assuming parallel and independent pathways for Q_β and Q_γ. The assumption is consistent with many observations reported in the literature (Adrian and Huang, 1984; Huang, 1986; Huang and Peachey, 1989; Chen and Hui, 1991*a*, *b*). The possible complications that might lead to an inaccuracy in using this method include the multi-component nature of Q_β and, perhaps, Q_γ. Q_β could consist of gating charges for various ionic channels and intramembranous charges that as yet have no known physiological role (Hui, 1991*b*). One piece of experimental evidence that supports this notion is the observation that Q_β has a nifedipine-sensitive and a nifedipine-resistant component (Chen and Hui, 1991*c*). Q_γ might also contain a component mobilized by the feedback of Ca release from the sarcoplasmic reticulum. However, the several-fold difference in the values of k for the two Boltzmann distribution functions obtained from curve fitting suggests that the grouping of different species of charge into two major Boltzmann components could be correct, to the lowest order of approximation.

Another source of error in this separation method is attributed to the scatter of data. A fitting of two Boltzmann distribution functions, with six adjustable parameters, to the data is particularly sensitive to the scatter. We have artificially incremented the value of one or two points in a *Q-V* plot by 1–2 nC/μF and observed a substantial increase in the value of $q_{\beta,max}/c_m$ or $q_{\gamma,max}/c_m$, depending on which point(s) in the plot was altered. Thus, a relatively small scatter in one or two points could lead to an undesirable error in the separation of the two charge components. Fortunately, except for the presence of ionic contamination, it is unlikely that the scatter in our cut fiber experiments could be as large as 2 nC/μF (although this amount of scatter is often present in intact fiber experiments). Thus, with this method of separation, the estimates for the Q_γ parameters should be more reliable than the Q_β parameters because the steeply rising portion of a *Q-V* plot that corresponds to the Q_γ component is less likely to be contaminated by ionic current. It is hoped that a statistical average of a large enough number of experiments can eliminate the uncertainty caused by the scatter, which should be random. In any event, with good quality data acquisition hardware and careful data processing, this method is by far the most useful and the simplest to use when both Q_β and Q_γ exist in substantial proportions. However, when one component exists in a small proportion, it cannot be separated easily because the fitting routine often does not converge.

Method 4. This method does not provide information about the absolute value of $q_{\gamma,max}/c_m$ or Q_β parameters. The method is based on the assumption that the decay time constant of I_γ during the post-pulse is independent of the potential during the TEST pulse. This assumption was supported by the experiment shown in Fig. 4 *B* of Hui and Chandler (1991), but the scatter of data in that experiment could easily obscure a weak voltage dependence of the time constant. Another complication is that, when method 3 is used, an OFF charge contaminated by ionic current can be replaced by an ON charge in a *Q-V* plot, provided that a baseline can be fitted reliably to the ON segment. With method 4, such replacement is not valid.

If method 4 is used to study the effect of an intervention, such as the application of tetracaine, on Q_γ, a change of the time constant by the intervention can yield erroneous conclusions. However, if the Q_γ component is too small to be separated by method 3, this method can be used as a remedy. An example of this backup use of

method 4 to supplement method 3 will be presented in the following paper (Hui and Chen, 1992).

Blockage of Charge Movement by Tetracaine

Results presented in this paper show convincingly that the I_γ hump in the ON segments of TEST-minus-CONTROL current traces from cut fibers can be blocked by tetracaine (Figs. 1, 2, 4, 7, and 8); the same is true for the slow I_γ component in the OFF current at around −60 mV (Figs. 7 and 8). By separating Q_β and Q_γ with method 3, the individual dose–response relationships for the blockage of Q_β and Q_γ by tetracaine were obtained (Table I). Because of the uncertainties in the separation method, as described in the preceding section, the reduction in the amount of Q_β is too small to post an effect of tetracaine on Q_β. A lack of effect of tetracaine on Q_β would be in agreement with the finding of Almers and Best (1976) in frog intact fibers or with that of Hollingworth et al. (1990) in rat intact fibers bathed in an isotonic solution.

In contrast to the negative effect of tetracaine on Q_β, submillimolar concentrations of the drug have profound effects on Q_γ. Even 0.5 mM tetracaine can block as much as two-thirds of Q_γ on average, or 100% in a couple of fibers. Vergara and Caputo (1983) used the same concentration of the drug to block apparently all of Q_γ. This is surprisingly different from the results obtained from intact fibers. Huang (1982) and Hui (1983*a*) had to use 2–4 mM of the drug to suppress Q_γ substantially in intact fibers. Specifically, 2 mM blocks about half of Q_γ in intact fibers (Hui, 1983*b*). Thus, when acted on by tetracaine, intact and cut fibers apparently have quite different dose responses, which could be related to possible differences in the physiological states of the two preparations. A similar diversity in the dose dependence of drug action was seen with nifedipine (in intact fibers: Lamb, 1986; Huang, 1990; in cut fibers: Rios and Brum, 1987; Chen and Hui, 1991*c*).

Although 25 μM is too low a concentration for tetracaine to exert any blocking action on Q_γ, it reveals an interesting effect in shifting the Q_γ-V curve in the depolarizing direction. The shift is not surprising, as a much larger shift of the K conductance versus voltage curve by 2 mM tetracaine was observed in intact fibers (Almers, 1976). The dose dependence of the shift in $\overline{V}_\gamma$ by tetracaine has not been studied.

Csernoch et al. (1989) observed difference charge movement traces similar to those in Fig. 2 *C* and difference Q-V plots similar to that in Fig. 6 *A*. They utilized the results as evidence to support the hypothesis that Q_γ is a consequence of Ca release from the SR. We have shown here that those features can be explained simply by a voltage shift in the Q-V distribution and in the voltage dependence of the kinetics of I_γ. If the TEST potential is so chosen that the I_γ hump is pronounced and the kinetics of the hump is not too fast to make it fuse with I_β, the potential will probably fall on the steep portion of the Q-V curve. Then a shift of the Q-V curve by just a few millivolts to the right will make it appear that Q_γ is suppressed, even though it is actually not, and will also generate the biphasic waveform in the charge movement traces.

Parallel Pathways for Q_β and Q_γ

It is amazing that the four separation methods, based on entirely different principles, can yield Q_γ components that are in such good qualitative agreement with each other. With these results, we are confident that the intramembranous charge in skeletal muscle can be divided, to the first order of approximation, into two groups, one with a steep and the other with a more shallow voltage dependence. We can also justify the identification of the charge carried by the slow ON and OFF transients in TEST-minus-CONTROL current traces with the steeply voltage-dependent charge component and with the tetracaine-sensitive charge component.

The results presented in this paper do not provide information about how Q_β and Q_γ are related to each other, nor about how Q_β or Q_γ triggers Ca release from the SR. However, on other occasions we have shown that Q_β and Q_γ cannot be tightly coupled to each other in a sequential manner (Chen and Hui, 1991*a*, *b*; Hui and Chandler, 1991), although fractions of Q_β and Q_γ can. It is possible that Q_β might not play any role in excitation–contraction coupling (see Discussion in Hui, 1991*b*), which is entirely speculative, and supporting evidence for this idea remains to be collected.

The steep voltage dependence of Q_γ, obtained independently by four separate methods, correlates very well with the steep voltage dependence of the maximum rate of Ca release (Baylor et al., 1983; Melzer et al., 1986; Maylie et al., 1987). The results thus reestablish the strong association of Q_γ with Ca release. However, the experiments were not designed to differentiate whether Q_γ triggers Ca release, as suggested by Huang (1982), Hui (1983*b*), and Vergara and Caputo (1983), or Q_γ arises totally from the feedback of Ca release (Csernoch et al., 1989; Pizarro et al., 1990). Some speculation along this line was presented in a previous paper (Hui, 1991*a*) and will not be repeated here. Recently, this controversy has attracted a lot of attention from investigators and is not likely to be resolved without great effort in the future. In any case, whether Q_γ is the cause or the result of Ca release, most of us will agree that it is an important signal in the excitation–contraction coupling sequence. Hence, it is preferable to develop a reliable technique to separate it from the total charge. This paper provides some insight in this direction.

This project was supported by grants from the National Institutes of Health (NS-21955) and the Muscular Dystrophy Association. C. S. Hui was a recipient of a Research Career Development Award (NS-00976) from the NIH and W. Chen was a recipient of a postdoctoral fellowship from the Indiana Heart Association.

Original version received 29 April 1991 and accepted version received 23 January 1992.

REFERENCES

Adrian, R. H., and W. Almers. 1976. Charge movement in the membrane of striated muscle. *Journal of Physiology.* 254:339–360.

Adrian, R. H., W. K. Chandler, and R. F. Rakowski. 1976. Charge movement and mechanical repriming in skeletal muscle. *Journal of Physiology.* 254:361–388.

Adrian, R. H., and C. L.-H. Huang. 1984. Experimental analysis of the relationship between charge movements in skeletal muscle of Rana temporaria. *Journal of Physiology.* 353:419–434.

Adrian, R. H., and A. R. Peres. 1977. A gating signal for the potassium channel? *Nature.* 267:800–804.

Adrian, R. H., and A. R. Peres. 1979. Charge movement and membrane capacity in frog muscle. *Journal of Physiology*. 289:83–97.

Almers, W. 1976. Differential effects of tetracaine on delayed potassium channels and displacement currents in frog skeletal muscle. *Journal of Physiology*. 262:613–637.

Almers, W., and P. M. Best. 1976. Effects of tetracaine on displacement currents and contraction of frog skeletal muscle. *Journal of Physiology*. 262:583–611.

Baylor, S. M., W. K. Chandler, and M. W. Marshall. 1983. Sarcoplasmic reticulum calcium release in frog skeletal muscle fibers estimated from arsenazo III calcium transients. *Journal of Physiology*. 344:625–666.

Chandler, W. K., and C. S. Hui. 1990. Membrane capacitance in frog cut twitch fibers mounted in a double Vaseline-gap chamber. *Journal of General Physiology*. 96:225–256.

Chandler, W. K., R. F. Rakowski, and M. F. Schneider. 1976*a*. A nonlinear voltage dependent charge movement in frog skeletal muscle. *Journal of Physiology*. 254:245–283.

Chandler, W. K., R. F. Rakowski, and M. F. Schneider. 1976*b*. Effects of glycerol treatment and maintained depolarization on charge movement in skeletal muscle. *Journal of Physiology*. 254:285–316.

Chen, W., and C. S. Hui. 1989. Effects of tetracaine and maintained depolarization on charge movement components in frog cut twitch fibers. *Biophysical Journal*. 55:239*a*. (Abstr.)

Chen, W., and C. S. Hui. 1991*a*. Existence of Q_γ in frog cut twitch fibers with little Q_β. *Biophysical Journal*. 59:503–507.

Chen, W., and C. S. Hui. 1991*b*. Gluconate suppresses Q_β more effectively than Q_γ in frog cut twitch fibers. *Biophysical Journal*. 59:543*a*. (Abstr.)

Chen, W., and C. S. Hui. 1991*c*. Differential blockage of charge movement components in frog cut twitch fibres by nifedipine. *Journal of Physiology*. 444:579–603.

Csernoch, L., C. L.-H. Huang, G. Szucs, and L. Kovacs. 1988. Differential effects of tetracaine on charge movement and Ca^{2+} signals in frog skeletal muscle. *Journal of General Physiology*. 92:601–612.

Csernoch, L., I. Uribe, M. Rodriguez, G. Pizzaro, and E. Rios. 1989. Q_γ and Ca release flux in skeletal muscle fibers. *Biophysical Journal*. 55:88*a*. (Abstr.)

Hollingworth, S., M. W. Marshall, and E. Robson. 1990. The effects of tetracaine on charge movement in fast twitch rat skeletal muscle fibres. *Journal of Physiology*. 421:633–644.

Horowicz, P., and M. F. Schneider. 1981. Membrane charge movement in contracting and non-contracting skeletal muscle fibres. *Journal of Physiology*. 314:565–593.

Huang, C. L.-H. 1982. Pharmacological separation of charge movement components in frog skeletal muscle. *Journal of Physiology*. 324:375–387.

Huang, C. L.-H. 1986. The differential effects of twitch potentiators on charge movements in frog skeletal muscle. *Journal of Physiology*. 380:17–33.

Huang, C. L.-H. 1990. Voltage-dependent block of charge movement components by nifedipine in frog skeletal muscle. *Journal of General Physiology*. 96:535–557.

Huang, C. L.-H., and L. D. Peachey. 1989. Anatomical distribution of voltage-dependent membrane capacitance in frog skeletal muscle fibers. *Journal of General Physiology*. 93:565–584.

Hui, C. S. 1982. Pharmacological dissection of charge movement in frog skeletal muscle fibers. *Biophysical Journal*. 39:119–122.

Hui, C. S. 1983*a*. Pharmacological studies of charge movement in frog skeletal muscle. *Journal of Physiology*. 337:509–529.

Hui, C. S. 1983*b*. Differential properties of two charge components in frog skeletal muscle. *Journal of Physiology*. 337:531–552.

Hui, C. S. 1991*a*. Comparison of charge movement components in intact and cut twitch fibers of the frog. Effects of stretch and temperature. *Journal of General Physiology*. 98:287–314.

Hui, C. S. 1991*b*. Factors affecting the appearance of the slow charge component in frog cut twitch fibers. *Journal of General Physiology*. 98:315–347.

Hui, C. S., and W. K. Chandler. 1990. Intramembranous charge movement in frog cut twitch fibers mounted in a double Vaseline-gap chamber. *Journal of General Physiology*. 96:257–297.

Hui, C. S., and W. K. Chandler. 1991. Comparison of Q_β and Q_γ charge movement in frog cut twitch fibers. *Journal of General Physiology*. 98:429–464.

Hui, C. S., and W. Chen. 1992. Effects of conditioning depolarization and repetitive stimulation on charge movement components in frog cut twitch fibers. *Journal of General Physiology*. 99:1017–1043.

Irving, M., J. Maylie, N. L. Sizto, and W. K. Chandler. 1987. Intrinsic optical and passive electrical properties of cut frog twitch fibers. *Journal of General Physiology*. 89:1–40.

Kovacs, L., E. Rios, and M. F. Schneider. 1983. Measurement and modification of free calcium transients in frog skeletal muscle fibres by a metallochromic indicator dye. *Journal of Physiology*. 343:161–196.

Lamb, G. D. 1986. Components of charge movement in rabbit skeletal muscle: the effect of tetracaine and nifedipine. *Journal of Physiology*. 376:85–100.

Maylie, J., M. Irving, N. L. Sizto, and W. K. Chandler. 1987. Calcium signals recorded from cut frog twitch fibers containing antipyrylazo III. *Journal of General Physiology*. 89:83–143.

Melzer, W., M. F. Schneider, B. J. Simon, and G. Szucs. 1986. Intramembrane charge movement and calcium release in frog skeletal muscle. *Journal of Physiology*. 373:481–511.

Murray, B. G. 1979. Population Dynamics: Alternative Models. Academic Press, New York.

Pizarro, G., M. Rodriguez, L. Csernoch, and E. Rios. 1990. Positive feedback in skeletal muscle E-C coupling. *Biophysical Journal*. 73:401*a*. (Abstr.)

Rios, E., and G. Brum. 1987. Involvement of dihyropyridine receptors in excitation-contraction coupling in skeletal muscle. *Nature*. 325:717–720.

Schneider, M. F., and W. K. Chandler. 1973. Voltage dependent charge movement in skeletal muscle: a possible step in excitation-contraction coupling. *Nature*. 242:244–246.

Vergara, J., and C. Caputo. 1983. Effects of tetracaine on charge movements and calcium signals in frog skeletal muscle fibers. *Proceedings of the National Academy of Sciences, USA*. 80:1477–1481.